AD-A045 527 MONTANA ENERGY AND MHD RESEARCH AND DEVELOPMENT INST --ETC F/G 11/2
THERMAL CONDUCTIVITY AND DIFFUSIVITY OF ENGINEERING CERAMICS.(U)
JUN 77 D P HASSELMAN, G E YOUNGBLOOD N00014-76-C-0884
UNCLASSIFIED NL

1 OF 2
ADA045 527

FINAL TECHNICAL REPORT

THERMAL CONDUCTIVITY AND DIFFUSIVITY OF ENGINEERING CERAMICS

D.P.H. HASSELMAN

G.E. YOUNGBLOOD

MONTANA ENERGY AND MHD
RESEARCH AND DEVELOPMENT INSTITUTE

JUNE 30, 1977

Prepared for:
DEPARTMENT OF THE NAVY
Office of Naval Research
Arlington, Virginia 22217

AGREEMENT NO.: N00014-76-C-0884

419:77F08

FINAL TECHNICAL REPORT

THERMAL CONDUCTIVITY AND DIFFUSIVITY OF ENGINEERING CERAMICS

D.P.H. Hasselman

G.E. Youngblood

MONTANA ENERGY and MHD

RESEARCH AND DEVELOPMENT INSTITUTE,

Butte.

June 30, 1977

Prepared for:

DEPARTMENT OF THE NAVY

Office of Naval Research
Arlington, Virginia 22217

Agreement No.: N00014-76-C-0884

Unclassified

SECURITY CLASSIFICATION OF THIS PAGE (When Data Entered)

REPORT DOCUMENTATION PAGE		READ INSTRUCTIONS BEFORE COMPLETING FORM
1. REPORT NUMBER	2. GOVT ACCESSION NO.	3. RECIPIENT'S CATALOG NUMBER
4. TITLE (and Subtitle) THERMAL CONDUCTIVITY AND DIFFUSIVITY OF ENGINEERING CERAMICS.		5. TYPE OF REPORT & PERIOD COVERED Final Technical Report. July 1976 — June 1977,
		6. PERFORMING ORG. REPORT NUMBER
7. AUTHOR(s) D.P.H. Hasselman, G. E. Youngblood		8. CONTRACT OR GRANT NUMBER(s) N00014-76-C-0884
9. PERFORMING ORGANIZATION NAME AND ADDRESS Montana Energy and MHD R. & D. Inst. Box 3809 Butte, Montana 59701		10. PROGRAM ELEMENT, PROJECT, TASK AREA & WORK UNIT NUMBERS 30 June 77
11. CONTROLLING OFFICE NAME AND ADDRESS Department of the Navy Office of Naval Research Arlington, VA. 22217		12. REPORT DATE June 30, ~~August~~ 1977
		13. NUMBER OF PAGES ~~105~~ 12 114
14. MONITORING AGENCY NAME & ADDRESS (if different from Controlling Office)		15. SECURITY CLASS. (of this report) Unclassified
		15a. DECLASSIFICATION/DOWNGRADING SCHEDULE

16. DISTRIBUTION STATEMENT (of this Report)

See distribution list. ~~Do Not Release~~

DISTRIBUTION STATEMENT A
Approved for public release;
Distribution Unlimited

17. DISTRIBUTION STATEMENT (of the abstract entered in Block 20, if different from Report)

18. SUPPLEMENTARY NOTES

19. KEY WORDS (Continue on reverse side if necessary and identify by block number)

Thermal conductivity, thermal diffusivity, thermal stress resistance, thermal conductivity gradient, micro-cracking, aluminum niobate, fibrous alumina, glass ceramics, alumina/zirconia composites

20. ABSTRACT (Continue on reverse side if necessary and identify by block number)

-OVER-

392916

DD FORM 1 JAN 73 1473 EDITION OF 1 NOV 65 IS OBSOLETE

Unclassified

SECURITY CLASSIFICATION OF THIS PAGE (When Data Entered)

This report summarizes the results of a one-year extension of a research program devoted to an investigation of the effect of compositional and microstructural variables on the thermal conductivity/diffusivity and thermal stress resistance of engineering ceramics. A total of six completed studies have resulted during this extension, with a seventh in preparation, as follows:

1. Thermal Diffusivity of Microcracked Ceramic Materials.
2. Thermal Diffusivity and Thermal Conductivity of a Fibrous Alumina.
3. Thermal Diffusivity/Conductivity of Alumina with a Zirconia Dispersed Phase.
4. Effect of Crystallization on the Thermal Diffusivity of a Mica Glass-Ceramic.
5. Effect of Microcracking on the Thermal Diffusivity of Polycrystalline Aluminum Niobate.
6. Enhanced Thermal Stress Resistance of Structural Ceramics with Thermal Conductivity Gradient.
7. Effect of Crystallization on the Thermal Diffusivity of a Cordierite Glass-Ceramic.

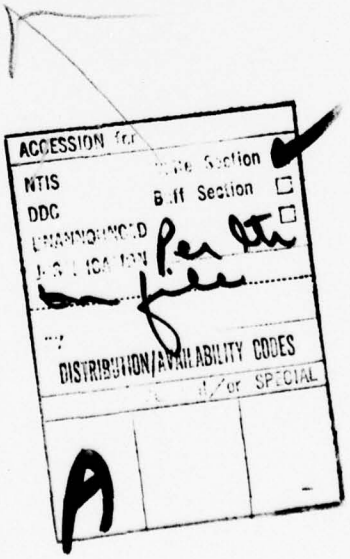

TABLE OF CONTENTS

TITLE: Thermal Conductivity and Diffusivity of Engineering Ceramics

I. INTRODUCTION

Ceramics, because of their high chemical inertness, high melting point, high hardness, excellent mechanical stability at high temperature and other unique properties, represent a class of materials which is eminently suited for many critical engineering applications.

The reliable engineering design and satisfactory performance of ceramic materials depend strongly on a detailed quantitative understanding of the pertinent physical properties which control their performance. The properties may include tensile and compressive strength, optical transparency and emissivity, hardness, thermal expansion and resistance to impact, mechanical and thermal fatigue and deformation by creep at high temperature. In particular, thermal conductivity and diffusivity can effect vitally the suitability of ceramics for many design applications.

Probably the best example of the importance of thermal conductivity in the performance of ceramics is in the area of thermal stress fracture under conditions of severe transient or steady-heat transfer (as encountered by turbine blades, radomes, nozzles, spark-plugs, crucibles, electrodes and numerous industrial and consumer products).[1-4]

Under these conditions, the magnitude of the temperature gradients and resulting values of thermal stress are dictated by values of thermal conductivity and/or thermal diffusivity of the particular ceramic. It is obvious that engineering calculations of the magnitudes of thermal stresses require reliable engineering data for the thermal conductivity and diffusivity of the ceramic being considered. Also, since thermal stress resistance requires ceramics with values of thermal conductivity as high as possible, an understanding of the underlying factors which control

conductivity is important. This understanding should indicate methods to improve thermal conductivity through microstructural control, composite development, purity control and other techniques.

High thermal conductivity is also a desirable feature of ceramic materials used in electronic applications such as substrates, as well as ceramic materials subjected to wear and abrasion. In contrast, ceramics used in manufacturing and research equipment, which require high temperature insulation properties, should have low values of thermal conductivity, primarily for the purpose of keeping energy requirements to a minimum.

Thermal conductivity also plays a major role in governing the design of nuclear reactors, super- and hypersonic aircraft, wind tunnels, heat exchangers, space-craft such as re-entry vehicles, power generation devices and numerous other engineering structures operating at temperatures above or below ambient. Thermal diffusivity directly plays a major role when components must operate in a rapidly changing (transient) temperature environment. Even from the few examples given above, it is clear that thermal conductivity and thermal diffusivity are of major importance in the engineering performance of ceramics in a wide variety of industrial and scientific applications.

In general, thermal transport properties of a solid are controlled by inter-atomic [1,5,6] as well as microstructural, compositional and other variables. Heat conduction can occur via phonon or electron transport as well as by internal radiation at higher temperatures. Ceramic materials with high thermal conductivities generally involve simple compounds between elements of low atomic weight with high heats of formation, high hardness and high elastic modulus. Examples include beryllium oxide, boron nitride, magnesium oxide, aluminum oxide, silicon carbide,

titanium carbide and others. However, apart from the choice of a given compound, the materials engineer has little or no control of the thermal transport properties determined by atomic variables. Thermal conductivity, fortunately, is controlled also by microstructural variables such as grain size, porosity, texture and impurity content. In addition, the presence of microcracks can profoundly affect the thermal conductivity as well as the fracture toughness and resistance to thermal shock damage. These variables are within the control of the materials engineer, especially in view of the many new ceramic processing techniques developed over the last few years in combination with the availability of markedly improved materials. As a result, much greater control over thermal conductivity can be exerted than was the case as little as a decade ago. However, to exercise such control it is important that the degree of the effect of microstructural, compositional and other variables on thermal conductivity be understood.

Therefore, the emphasis in this research program, carried out under the guidance of the principal investigator over the last three years, was to relate thermal transport properties through the measurement of the thermal diffusivity and its temperature dependence with controllable variables such as composition, microstructure, porosity, degree of crystallinity and impurity levels for a wide range of ceramic materials. A number of analytical studies were carried out as well. The purpose of this report is to present the results obtained during the past year.

II. EXPERIMENTAL PROCEDURE

The laser-flash diffusivity technique was selected as the primary method of determination of thermal transport properties. This method has been demonstrated to be rapid, convenient and to give reproducible results.[7-16] Furthermore, this technique uses a very small and simple specimen geometry. The major effort of the program then can be devoted

principally to the measurements of thermal properties, rather than to the time-consuming (and often highly expensive) preparation of specimens.

Specifically, for this program the laser used was of the glass-neodymium type (Korad #K-1) which fires a single pulse (pulse width of ≈800 nsec) of 1.06 μm radiation. The laser flash is directed at one face of a disc-shaped specimen, measuring 1/2 inch diameter by ≲0.1 inch thick and mounted on a suitable specimen holder within a cylindrical graphite chamber. In turn, the graphite chamber is contained in a high-temperature furnace (Astro Industries #1000) capable of attaining a temperature in excess of 2500°C. Specimens are coated with a thin layer of carbon in order to make them opaque to the laser radiation and to make the emmitance/absorptance characteristics of all specimens the same. The transient temperature response of the opposite face of the specimen is monitored either with an infrared (InSb) detector (Barnes Engineering #IT-7B) or with an chromel constantan thermocouple attached to the specimen with a small dab of ceramic cement. The transient signal from either detector is recorded on a storage oscilloscope (Tektronix #5111). All measurements were made in an inert atmosphere of dry nitrogen.

The thermal diffusivity (α) is calculated from the time ($t_{1/2}$) required for the temperature of the back-face of the specimen to reach half of its maximum value (also the steady-state value) from

$$\alpha = A\ell^2/t_{1/2} \qquad (1)$$

where ℓ is the specimen thickness and A is a dimensionless constant whose value depends on the rate of heat loss from the specimen during the time of measurement. Heat loss corrections were estimated to be less than 5% for all measurements. Since emphasis in this report is on relative changes in α due to controlled fabrication variables, heat loss corrections were

not made.

In order to promote research efficiency, the program was conducted in cooperation with scientists at other organizations. This cooperation took the form of the exchange of specimens so that this program could concentrate fully on the measurement and analysis of thermal transport properties without having to devote a major fraction of the program effort to specimen fabrication. At the same time, cooperating organizations obtained data and analysis of thermal transport properties for their materials. As a result both cooperating parties benefitted. Table I lists the cooperating organizations and the materials studied as part of this program.

III. SUMMARY OF RESULTS

Table II lists a total of 18 technical articles which have resulted from this program during the last three year period.[17,18] Complete reprints of six technical articles* covering experimental work completed within the past year appear as appendices. Additional data were obtained for the effect of microcracking on thermal diffusivity of polycrystalline aluminum-niobate. The technical article reporting the original data was rewritten to incorporate the new data. Brief summaries of the completed technical articles, including the rewritten aluminum niobate work, follow:

A. "Thermal Diffusivity of Microcracked Ceramic Materials."

This study reviews the effect of microcracking on the thermal diffusivity of iron titanate and magnesium dititanate reported previously together with new data for aluminum titanate. Data for these three materials together are compared and interpreted in terms of the effect

*Complete reprints of the other 12 technical articles appear as appendices in References 17 and 18.

of grain size on microcrack formation. All three materials exhibited different degrees of a pronounced hysteresis of the thermal diffusivity values depending on whether measurements were made during sample heating or cooling. This hysteresis was attributed to irreversible crack-healing and closure at the higher temperatures on heating followed by crack-reopening or new crack formation on cooling. This study will appear in the Proceedings of the Symposium on Ceramic Microstructures held in Berkeley, California, August, 1976.

B. "Thermal Diffusivity and Conductivity of a Fibrous Alumina."

This study concentrated on the measurement and interpretation of the heat transfer properties of fibrous alumina of various densities. The principle conclusion was that at a given density the pores in a fibrous microstructure are more effective in lowering the thermal diffusivity and conductivity of a ceramic material than the isolated isometric pores found in sintered or hot-pressed materials. This study was published in the American Ceramic Society Bulletin.

C. "Thermal Diffusivity/Conductivity of Alumina with a Zirconia Dispersed Phase."

This study investigated the effects of microcracking on the thermal diffusivity and conductivity of an alumina matrix containing a dispersed phase of non-stabilized zirconia. The microcracks are introduced into the alumina matrix on cooling after hot-pressing when the zirconia particles expand during the tetragonal to monoclinic phase-transformation. The experimental data indicated that the microcracking caused a significant decrease in the thermal conductivity and diffusivity over the total temperature range (R.T. to 800°C) with a complete absence of any hysteresis effect. This is in sharp contrast to the polycrystalline titanates which, as reported earlier, exhibit a pronounced thermal

diffusivity hysteresis on heating and cooling. The reason for this difference is that the microcracking in the polycrystalline titanates is due to the anisotropy in thermal expansion between grains which in turn leads to unavoidable crack-closure on reheating. For the alumina-zirconia, however, the microcracked structure is supported by the expanded monoclinic zirconia particles (below the phase transformation temperature). Once formed, the size and density of these microcracks apparently are independent of the degree of cooling such that a hysteresis in the thermal diffusivity/conductivity is not observed. The results from this study were presented at the 79th annual meeting of the American Ceramic Society in Chicago and were published in the American Ceramic Society Bulletin.

D. "Effect of Microcracking on the Thermal Diffusivity of Polycrystalline Aluminum Niobate."

This study presents experimental data illustrating the effect of microcracking on the thermal diffusivity of aluminum niobate from room temperature to about 750°C. In this study, the transient temperature change of the specimens was monitored with a thermocouple. These data agreed with previously reported data obtained with the use of the IR-detector from approximately 200°C to 1000°C. The new data were obtained primarily to investigate in detail the thermal diffusivity near room temperature. Data taken during successive temperature cycles suggest that the effect of microcracking on thermal diffusivity is maximum after the very first cooling from the fabrication temperature. Some permanent crack-healing persisted during subsequent heating and cooling. An explanation for this behavior is given in terms of the nature of unstable crack propagation in thermal strain fields. This study will be published in the Journal of the American Ceramic Society.

E. "Enhanced Thermal Stress Resistance of Brittle Ceramics with Thermal Conductivity Gradient."

The analytical study was based on the fact that the magnitude of thermal stress in a brittle material depends not only on the magnitude of the temperature difference involved but also on the temperature distribution. In principle then, it should be possible to reduce the magnitude of thermal stress by modification of the distribution of temperature. This can be accomplished by the formulation of materials with a thermal conductivity gradient. The validity of this hypothesis was demonstrated analytically for a hollow cylinder with a thermal conductivity gradient through the wall subjected to steady-state radially inward or outward heat flow. The numerical results obtained show that thermal conductivity gradients can result in significant reductions in thermal stress. This study has been accepted for publication in the Journal of the American Ceramic Society.

F. "Effect of Crystallization on the Thermal Diffusivity of a Mica Glass-Ceramic."

This study reports experimental data for the thermal diffusivity of mica glass-ceramics with increasing degrees of crystallization achieved as the result of heat-treatment over a range of temperatures. As expected, the crystallization resulted in an increase in the thermal diffusivity from the original value of the glass. This increase was maximum at room temperature and decreased with increasing temperature. An explanation for these observations is given in terms of the mean free paths for phonon and photon conduction. This study will be published in the American Ceramic Society Bulletin.

In addition to these completed works, experimental thermal diffusivity and density data were obtained for another glass-ceramic. The

analysis is complete enough so that a preliminary technical article has been prepared and is included in the"Work in Progress" section. A brief summary of the article follows.

G. "Effect of Crystallization on the Thermal Diffusivity of a Cordierite Glass-Ceramic."

This study is a follow-up on the study of the mica glass-ceramic reported in Appendix F. Its purpose was to investigate the effect of crystallization on the thermal diffusivity of a glass-ceramic whose crystalline phase is a form other than the mica-structure. The thermal conductivity of mica in a direction perpendicular to the basal planes, which are held together by Van der Waals bonding, is expected to be relatively low. For this reason the thermal diffusivity in a mica glass-ceramic will be affected little by those mica crystals whose basal planes are perpendicular to the direction of heat flow. Other glass-ceramics containing crystals with ionic or covalent bonding where no such orientation effect should exist are expected to show a much greater change in the thermal diffusivity than the glass-ceramics containing mica crystals. The validity of this hypothesis was confirmed by the thermal diffusivity data obtained for a cordierite glass-ceramic, whose crystalline phase is primarily ionic. The results will be submitted to the Journal of the American Ceramic Society.

IV. WORK IN PROGRESS

Additional thermal diffusivity data were obtained for other materials during the program extension period. At the end of the contractural period, further microstructural analysis was needed in most cases before a final interpretation could be reported and technical publications (in addition to the ones listed in Table II) prepared. However, some conclusions based on thermal diffusivity data alone can be reported. In order to present those conclusions at this time, the partially completed studies are described in this "Work in Progress" section.

A. "Effect of Crystallization on the Thermal Diffusivity of a Cordierite Glass-Ceramic."

The thermal conductivity of solids is controlled by the specific heat, density and the mean free path of the specific carriers such as phonons and photons responsible for the heat transfer. Glassy (non-crystalline) materials are expected to have a very short phonon mean free path in comparison to crystalline materials. As a result, at low and moderate temperatures at which phonon transport is the primary mechanism for heat transport, glassy materials exhibit generally much lower thermal conductivity and diffusivity than crystalline materials. For this reason, crystallization of glass to form a glass-ceramic is expected to cause a significant increase in the thermal conductivity and diffusivity. In a previous investigation, the effect of crystallization on the thermal diffusivity of a mica glass-ceramic demonstrated this.

In general, the relative effect of partial crystallization in an amorphous material on the heat transfer properties is expected to be a function of the degree of crystallization, the crystalline structure, the nature of the atomic bonding and other relevant properties of the specific crystalline phase(s) formed. The phonon mean free path and velocity are expected to be much smaller in a mica crystalline phase (especially across basal planes with Van der Waals bonding) than in a crystalline phase with primarily ionic and covalent bonds. The presence of the latter type of crystalline phase is expected to cause a greater relative increase of the thermal diffusivity of a glass-ceramic than a mica crystalline phase. In the present note this hypothesis is verified by comparing experimental data for the thermal diffusivity of a cordierite glass-ceramic with corresponding data for a mica glass-ceramic reported previously.

Cylindrical samples (1" high by 1/2" in diameter) of the original glass with the same composition as a commercial glass-ceramic * were heated in approximately 45 minutes to 820°C and held for 2 hours for crystallite nucleation. Different samples then were heated rapidly to a series of high temperatures where they were held for 8 hours in order to promote crystallite growth. The crystallite morphology resulting from each of these heat treatments will be studied by replication transmission electron microscopy and correlated with thermal diffusivity results. The thermal diffusivity was measured over the temperature range of room temperature to approximately 750°C by the laser-flash technique using the same equipment and procedures as used for the mica glass-ceramic experiment.

The experimental data for the thermal diffusivity of the original glass and the series of heat-treated glass-ceramics are presented in Figure 1. At the lower temperatures the partial crystallization has caused increases in the thermal diffusivity (primarily the phonon component) of up to a factor in excess of three. At the higher temperatures, where the photon contribution to the thermal diffusivity becomes noticeable in a glass, the relative effect of the crystallization decreases due to the increased photon scattering at the numerous glass-crystal interfaces. It should be noted that the data for the thermal diffusivity of the most fully crystallized glass-ceramic (1260°C) lie somewhat below the data for a commercial cordierite glass-ceramic. In part, this difference can be attributed to the difference in the heat schedule used for the crystallization process.

Comparison of the present data with those reported for the mica

---

*Corning Glass Works, C9606

glass-ceramic shows that the original glasses for both studies have about the same value for the thermal diffusivity. On crystallization, however, the increases in the thermal diffusivity obtained for the cordierite glass-ceramic are far greater than those for the mica glass-ceramic. This observation is in qualitative agreement with the original hypothesis that for a glass-ceramic a crystalline phase with ionic or covalent bonding is expected to be far more effective in increasing the thermal diffusivity of the glass-ceramic than a crystalline phase in part held together by Van der Waals bonding. Exact quantitative estimates of this phenomenon in terms of lattice-dynamical theory are beyond the scope of the present study. In general, however, the present data and those obtained for the mica glass-ceramic suggest that the thermal diffusivity of glass-ceramics can be tailored to specific values by careful control over composition and heat treatment.

B. "Silicon Nitride"

The effect of the amount of sintering aid (MgO) and density on the thermal diffusivity of hot-pressed silicon nitride, a potential ceramic turbine material, is being studied. In Table III are shown room temperature thermal diffusivity data for Si_3N_4 prepared with similar densities by researchers at Annawerk. The samples were all hot-pressed at 1720°C for 80 minutes except for two samples with 3% MgO additive. In this case, one sample was held at temperature for 20 minutes and the other for 120 minutes. The samples with 3% MgO have the highest thermal diffusivity (and thermal conductivity). Apparently, the relative amount of glassy or crystalline second-phase at the grain boundaries, which in turn depends on the details of the time-temperature fabrication history as well as on composition, plays an important role in affecting

thermal support. Microstructural examination of these materials is in progress. It is clear, however, that both a wide range and quite high values of thermal diffusivity are possible for Si_3N_4 depending on fabrication processes.

C. "Barium mica / Alumina Composites."

The physical properties of a composite material can be quite susceptible to texture as well as composition effects. For instance, inclusions of barium mica in the form of flakes (roughly 30 μm in diameter by 5 to 10 μm thick) enhance the mechanical properties of an alumina/mica composite. The addition of mica to alumina has a considerable effect on lowering the thermal diffusivity which makes them doubly useful for application where more thermal resistive properties are necessary. This is particularly the case when the mica additions are aligned so that all the flakes are nearly parallel.

Figure 2 shows the typical type of texture achieved in two dense aluminas with 5 and 30 vol % Ba mica additions. The lower magnifications reveal a homogeneous distribution of separated and aligned mica flakes. The higher magnifications show that the flakes are discrete and have not reacted with the alumina matrix. Figure 3 illustrates the thermal diffusivity and its temperature dependence for various compositions where the mica flakes lie preferentially perpendicular to the thermal conduction direction. As discussed in A. above, the thermal conductivity of mica in a direction perpendicular to its basal planes is expected to be lower than in a direction parallel to the basal planes. This would account somewhat for the effectiveness of the mica flakes in lowering the thermal diffusivity in Ba mica/alumina composites with texture when the thermal pulse is predominently normal to the mica flakes. Further analysis of the temperature dependence of the thermal diffusivity is in progress.

REFERENCES

1. W. D. Kingery, Introduction to Ceramics, John Wiley, 1960.

2. W. B. Crandall and J. Ging, Journal American Ceramic Society, 38, P. 44, 1955.

3. D. P. H. Hasselman, Journal American Ceramic Society, 46, p. 229, 1963.

4. D. P. H. Hasselman, American Ceramic Society Bulletin 49, p. 1033, 1970.

5. C. Kittel, Introduction to Solid State Physics, John Wiley, 1956.

6. A. J. Dekker, Solid State Physics, Prentice-Hall, 1958.

7. Thermal Conductivity, ed. by D. R. Blynn and B. A. Peary, Jr. NBS Special Publication, 302, 1968.

8. N. S. Rasor and J. D. McClelland, Review of Scientific Instruments, 31, p. 595, 1960.

9. W. J. Parker, R. J. Jenkins, C. P. Butler and G. L. Abbott, Journal Applied Physics, 32, p. 1679, 1961.

10. R. D. Cowan, Journal Applied Physics, 34, p. 926, 1963.

11. J. A. Cape and G. W. Lehman, Journal Applied Physics, 34, p. 1909, 1963.

12. R. E. Taylor and J. A. Cape, Applied Physics Letters, 5, p. 212, 1964.

13. D. Haw and L. A. Goldsmith, Journal Science Instruments, 43, p. 595, 1966.

14. C. C. Weeks, M. M. Nakata and C. A. Smith, Thermal Conductivity, NBS Special Publication 302, pp. 387-398, 1968.

15. S. Nasu, T. Takahashi and T. Kikuchi, Journal Nuclear Material, 43, p. 72, 1972.

16. B. Granoff, H. O. Pierson and D. M. Schuster, Journal Composite Material, 7, p. 36, 1973.

17. J. E. Matta, J. H. Siebeneck, B. K. Ganguly and D. P. H. Hasselman, Interim Technical Report, Department of the Navy (ONR), Agreement No. N00014-67-A-0370-0011.

18. J. H. Siebeneck and D. P. H. Hasselman, Final Technical Report, Department of the Navy (ONR), Agreement No. N00014-75-C-0760

TABLE I

Cooperating organizations and ceramic materials for thermal diffusivity studies.

Organizations	Materials
1. Pennsylvania State University	Microcracked materials Glassy carbons Non-stoichiometric TiO_2 Silicon carbides Aluminum oxides
2. Westinghouse Corporation	Sialons, SiYONs*
3. Fiber-Materials Inc.	Fibrous aluminas
4. Corning Glass	Glass-ceramics*
5. Champion Spark Plug	Microcracked aluminum niobate
6. Naval Research Labs	Glasses Silicon nitride/silica composites Aluminum oxide/boron nitride composites*
7. General Electric Corp.	Glass-ceramics Sialons
8. Max Planck Institute	Alumina/zirconia* Alumina/titanium carbide and Alumina/silicon carbide composites
9. Rockwell International	Si_3N_4-Y_2O_3-SiO_2
10. Aerospace Research Institute (DEVLR) Cologne, Germany	Si_3N_4-MgO* Reduction-sintered silicon nitride
11. AMMRC	Ba-mica/Al_2O_3 composites* Silica
12. Anna-Werk	Si_3N_4-MgO*
13. Philips (Eindhoven, Netherlands)	Polycrystalline aluminas
14. Union Carbide	Textured BN composites*
15. University of Utah	Doped alumina* Ta-doped rutile

TABLE I
(Continued)

Organizations	Materials
16. University of California	Metal/glass composites* (bonded and non-bonded)
17. United Technologies	Glass/Alumina fiber composites
18. Feldmuhle Corporation (Germany)	Polycrystalline aluminas
19. Lehigh University	Polycrystalline aluminas
20. Battelle Laboratories	Glass-ceramics
21. McMaster University (Canada)	Partially stabilized zirconia

*Work in progress on these materials.

TABLE II

List of publications which have resulted from technical effort to date -(May 15, 1975- July 1, 1977).

1. B. K. Ganguly, K. R. McKinney and D. P. H. Hasselman, "Thermal Stress Analysis of Flat Plate with Temperature Dependent Thermal Conductivity," Journal American Ceramic Society, 58, pp.455-56, 1975.

2. J. E. Matta and D. P. H. Hasselman, "The Thermal Diffusivity of Al_2O_3-Cr_2O_3 Solid Solutions," Journal American Ceramic Society, 58, p.458, 1975.

3. J. E. Matta, H. J. Siebeneck and D. P. H. Hasselman, "The Effect of Microstructure and Composition on the Thermal Diffusivity of Structural Ceramics," Proceedings 1975 Conference on Laser-Hardening of Materials and Structures, NASA-Ames Research Center, Moffat Field, California.

4. B. K. Ganguly and D. P. H. Hasselman, "Effect of Conductivity on the Radiation Heat Transfer Across Spherical Pores," Journal American Ceramic Society, 59, 1-2, p. 83, 1976.

5. H. J. Siebeneck, W. P. Minnear, R. C. Bradt and D. P. H. Hasselman, "Thermal Diffusivity of Non-Stoichiometric Titanium Dioxide," Journal American Ceramic Society, 59, 1-2, p. 84, 1976.

6. H. J. Siebeneck, J. J. Cleveland, D. P. H. Hasselman and R. C. Bradt, "Effect of Micro-Cracking on the Thermal Diffusivity of Fe_2TiO_5," Journal American Ceramic Society, 59, 5-6, pp. 241-44,1976.

7. F. F. Lange, J. J. Siebeneck and D. P. H. Hasselman, "Thermal Diffusivity of Four Si-Al-O-N Compositions," Journal American Ceramic Society, 59, 9-10, pp. 454-55, 1976.

8. J. E. Matta, W. L. Roper, D. P. H. Hasselman and G. E. Kane, "The Role of Thermal Diffusivity in the Machining Performance of Oxide Ceramic Cutting Tool Materials," Wear, 31, pp. 323-32, 1976.

9. D. P. H. Hasselman, "Microcracking as a Mechanism for Improving Thermal Shock Resistance and Thermal Insulating Properties of Ceramic Materials," High Temperature - High Pressure (in press). Also presented at the 5th European Conference on Thermophysical Properties of Solids at High Temperature, Moscow, May 18-21, 1976.

10. H. J. Siebeneck, J. J. Cleveland, D. P. H. Hasselman and R. C. Bradt, "Thermal Diffusivity of Microcracked Ceramic Materials," presented at the Symposium on Ceramic Microstructures, Berkeley, California, August 23-27, 1976 (in press).

11. H. J. Siebeneck, J. J. Cleveland, D. P. H. Hasselman and R. C. Bradt, "Effect of Microcracking on the Thermal Diffusivity of $MgTi_2O_5$," Journal American Ceramic Society, (in press).

TABLE II (Continued)

12. H. J. Siebeneck, R. A. Penty, D. P. H. Hasselman and G. E. Youngblood, "Thermal Diffusivity and Thermal Conductivity of a Fibrous Alumina." Ceramic Bulletin, 56, 6, p. 572, 1977.

13. D. Greve, N. Claussen, D. P. H. Hasselman and G. E. Youngblood, "Thermal Diffusivity/Conductivity of Alumina with a Zirconia Dispersed Phase," Ceramic Bulletin, 56, 5, p. 414, 1977.

14. H. J. Siebeneck, E. J. Minford, P. A. Urick, D. P. H. Hasselman and R. C. Bradt, "Thermal Diffusivities of Glassy Carbon," Carbon (in press).

15. H. J. Siebeneck, K. Chyung, D. P. H. Hasselman and G. E. Youngblood, "Effect of Crystallization on the Thermal Diffusivity of a Mica Glass-Ceramic," Journal American Ceramic Society, (in press).

16. G. E. Youngblood, W. R. Manning and D. P. H. Hasselman, "Effect of Microcracking on the Thermal Diffusivity of Polycrystalline Aluminum Niobate," (submitted to Journal American Ceramic Society).

17. D. P. H. Hasselman and G. E. Youngblood, "Enhanced Thermal Stress Resistance of Brittle Ceramics with Thermal Conductivity Gradient," Journal American Ceramic Society, (in press).

18. G. E. Youngblood, K. Chyung and D. P. H. Hasselman, "Effect of Crystallization on the Thermal Diffusivity of a Cordierite Glass-Ceramic," (in preparation).

TABLE III

Room temperature thermal diffusivity of Si_3N_4 with MgO additive.†

w/o MgO	density (gm/cc)	thermal diffusivity (cm^2/sec)
0	3.12	$0.13_7 \pm 0.010$
1	3.17	0.11_9
3	3.21	0.16_6
3*	3.20	0.15_7
3**	3.21	0.14_2
5	3.20	0.12_6
7	3.19	0.13_0

† Hot-pressed at 1720°C for 80 minutes.

* Hot-pressed at 1720°C for 120 minutes.

** Hot-pressed at 1720°C for 20 minutes.

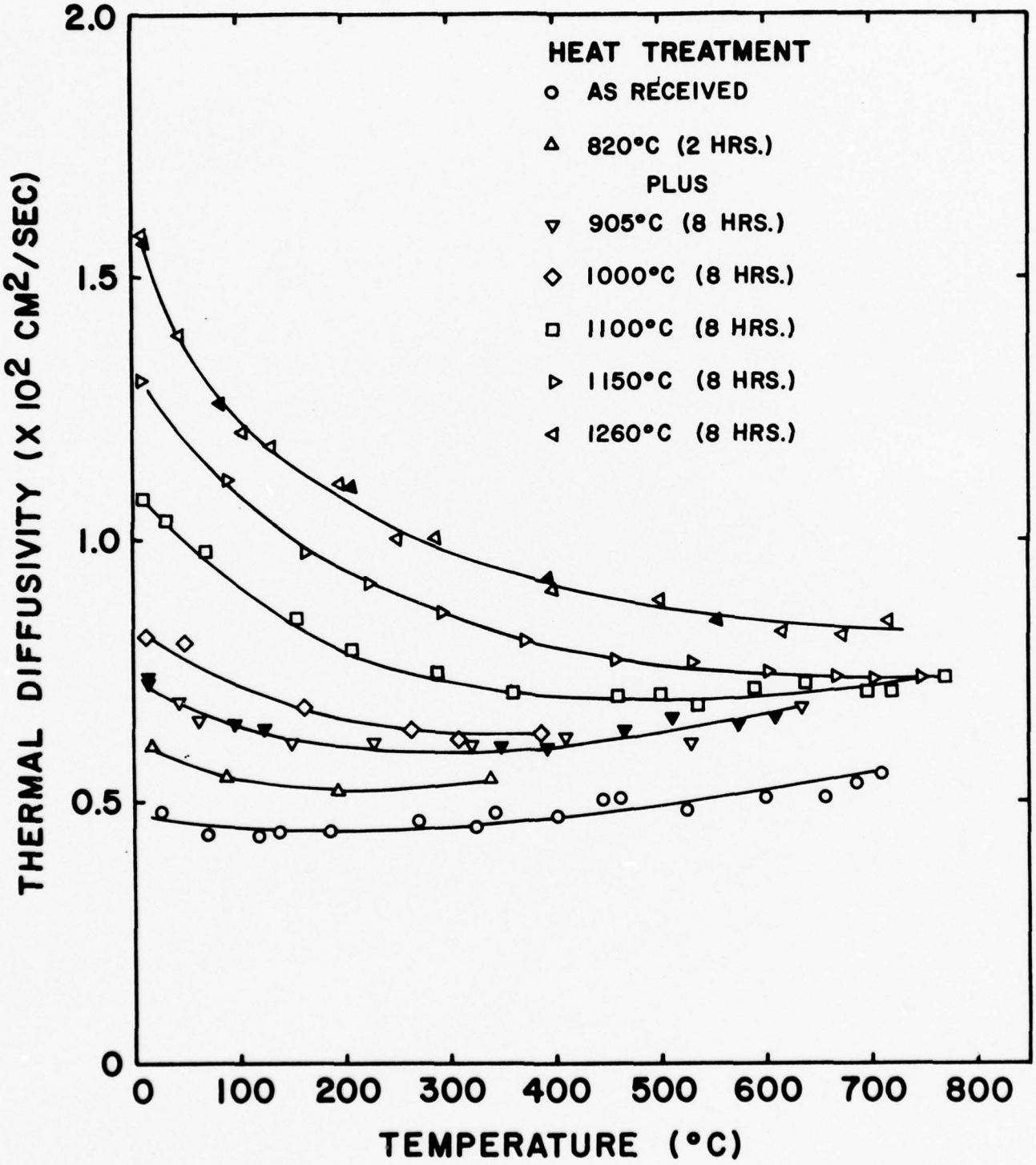

Fig. 1 Effect of crystallization on the thermal diffusivity of a Cordierite Glass-Ceramic. (open (solid) symbols indicate measurements made during heating (cooling).

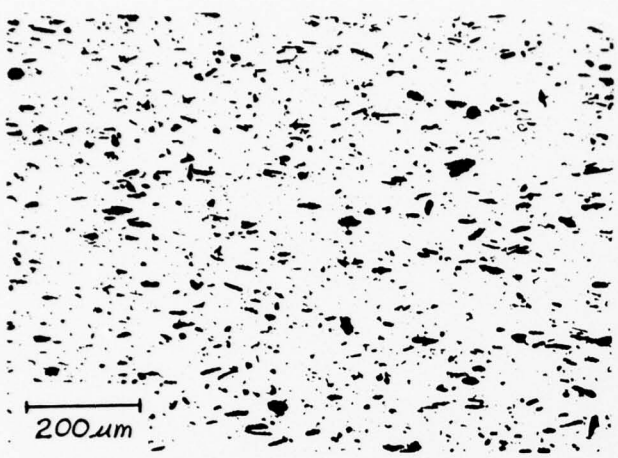

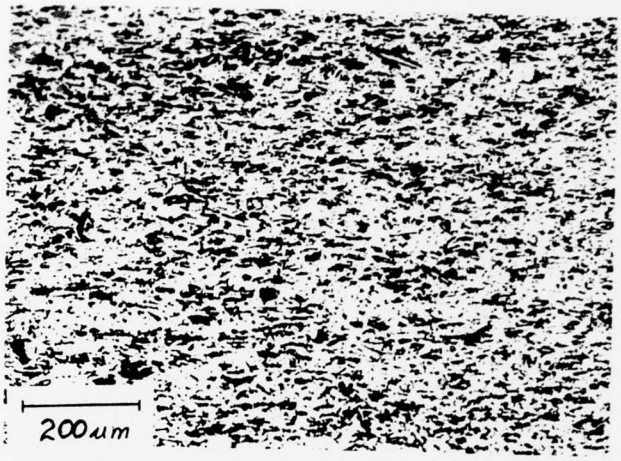

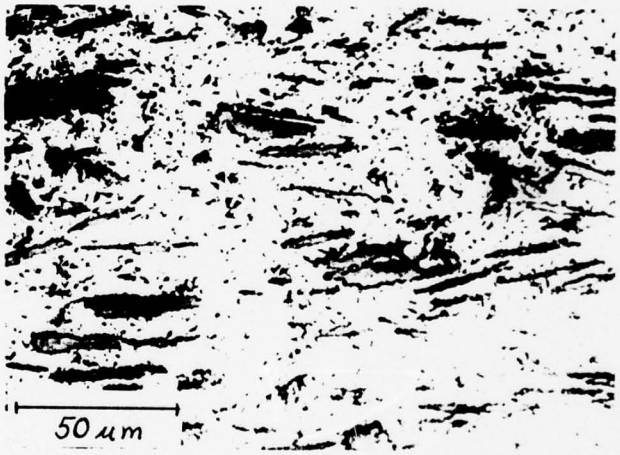

Fig. 2a

Fig. 2b

Fig. 2 Photomicrographs of Ba mica / Alumina Composites. Multiple relief polishing. Fig. 2a is 5 vol % 30 μm Ba mica in alumina at two magnifications. Fig. 2b is 30 vol % 30 μm Ba mica in alumina at two magnifications.

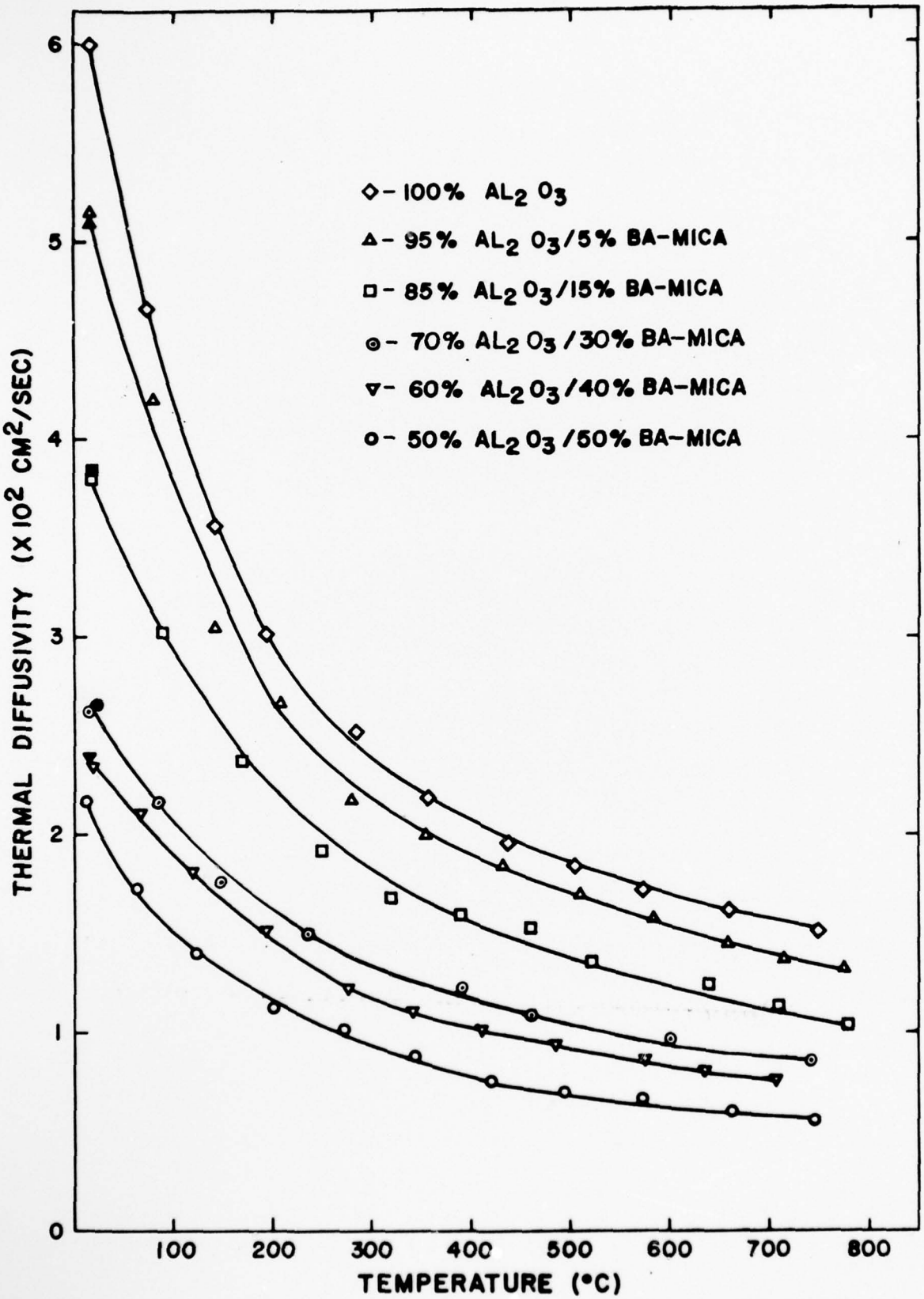

FIG. 3 THERMAL DIFFUSIVITY OF ALUMINA & ALUMINA/BA MICA COMPOSITES

APPENDIX A

THERMAL DIFFUSIVITY OF MICROCRACKED CERAMIC MATERIALS

THERMAL DIFFUSIVITY OF MICROCRACKED CERAMIC MATERIALS

by

H. J. Siebeneck*
J. J. Cleveland+
D. P. H. Hasselman§
R. C. Bradt+

Presented at the Symposium on Ceramic Microstructures
Berkeley, California, August 23-27, 1976

* University of Maryland, College Park, MD, 20740
+ Ceramic Science Section, Department of Materials Science, Pennsylvania State University, University Park, PA, 16803
§ The Montana Engergy and MHD Research and Development Institute Inc., Butte, MT. 59701

I. Introduction

The range of ceramic materials available today includes good thermal conductors as well as excellent thermal insulators. It is well known that thermal conductivity and thermal diffusivity of ceramics depend strongly on such microstructural variables as porosity (including total pore content, pore size, and shape), amount of glassy phase at grain boundaries, or the degree of crystallinity in such materials as glass-ceramics. Grain boundaries, as well as impurities or second-phase additions, can act as scattering centers for heat transfer by electron or phonon transport or by thermal radiation. The relative contributions of these latter mechanisms to the thermal conductivity (diffusivity) is a function of temperature and affects the absolute value of the thermal conductivity (diffusivity) as well as its temperature dependence.

Microcracking is an additional microstructural feature commonly observed for many ceramic materials. Such microcracking is expected to have a significant effect on thermal conductivity (diffusivity). Microcracked ceramics are of current and potential technical interest in view of their very low or even negative coefficient of thermal expansion. [1,2,3] Also, because of their high strains-at-fracture (ratio of tensile strength to Young's modulus) and their stable nature of crack propagation, microcracked ceramics exhibit exceptional thermal shock resistance. This has been demonstrated both experimentally [4,5] and analytically.[6,7] The beneficial effect of microcracking on fracture toughness [2] also should contribute to an improvement in thermal shock resistance and possibly impact resistance as well. Furthermore, microcracked ceramics exhibit elastic moduli which are unusually low compared to non-microcracked materials.

Microcracking in ceramic materials can be induced by a variety of

mechanisms. In non-cubic polycrystalline ceramics, microcracking can arise from a high degree of thermal expansion anisotropy. [8,9,10] Differences in the coefficient of the individual components in composites also can lead to the formation of microcracks, [4,11,12,13] as can volume changes [5] during crystallographic transformations.

The physical properties of many microcracked materials often exhibit an unusual temperature dependence. The strength and elastic moduli often increase strongly with increasing temperature. [1,2] On cooling, a very pronounced hysteresis effect often is found. Such hysteresis effects are thought to be related to frictional effects during crack opening and closure on thermal cycling or to crack healing at sufficiently high temperatures. Of particular interest is that the degree of microcracking and the resulting change to the physical properties appears to be a function of grain size. The magnitude of the internal stress responsible for the microcracking, however, is independent of the grain size. This suggests that microcracking is controlled not only by the level of stress but also by the strain-energy [2] or other variables.

An understanding of the effect that microcracking has on the heat transfer properties is required for purposes of material selection. The purpose of this paper is to present a summary and interpretation of recent experimental results for the thermal diffusivity of selected microcracked ceramics.

II. Experimental

A. Materials and Preparation

The three materials selected for the study were magnesium dititanate, iron titanate, and aluminum titanate. Polycrystalline samples for these materials exhibit microcracking due to the thermal expansion anisotropy of the individual grains.

Powders for these three titanates were prepared by the soild state reactions between the appropriate oxide powders. These powders were mixed by wet-milling in toluene-methanol media for 24 hours, then dried and fired in air at appropriate temperatures and times until the X-ray patterns agreed with literature data and no evidence of the original powders could be found. The powders then were screened to -25 mesh, dried, and hot-pressed in graphite dies at appropriate temperatures to within a few percent of the theoretical densities. Samples were cut from the hot-pressed billet and annealed for various times and temperatures (which are reported later) to promote grain-growth and to vary the degree of microcracking. The microstructure and evidence for microcracking were studied by scanning electron micrography of fracture surfaces.

B. Measurement of Thermal Diffusivity

The thermal diffusivity was measured by the laser-flash technique.[16] Specimens cut from the hot-pressed billet in the form of 1/2-inch diameter discs approximately 0.1 inch thick were held within a suitable graphite specimen holder inside a vertical carbon resistance furnace* with nitrogen atmosphere. The specimen faces were coated with carbon§ to

---

* Model 1000A Astr. Industries, Santa Barbara, California
§ Miracle DFG Spray, Miracle Power Products, Cleveland, Ohio

prevent direct transmission of the 1.06μm radiation from the glass-Nd laser.[+]

Thermal diffusivity measurement consisted of subjecting one face of the specimen to a single laser-flash through a quartz window at the top of the furnace. The transient temperature response of the opposite face of the specimen was monitored by either of two methods. The first method, used for the iron titanate specimen, employed an infrared detector[**] focused on the specimen surface through a second quartz window at the other end of the furnace. For the magnesium dititanate and the aluminum titanate, the transient temperature of the back surface was measured with a thermocouple attached to the specimen surface with a small amount of ceramic cement.[§§] The output signal of the IR-detector or the thermocouple was displayed on the screen of an oscilloscope equipped with signal storage.[++] Thermal diffusivity (α) was calculated from the specimen thickness (L) and the time ($t_{1/2}$) for the back-surface temperature of the specimen to reach one-half the value of the final uniform specimen temperature from

$$\alpha = 1.38L^2/\pi^2 t_{1/2}. \qquad (1)$$

The ambient temperature of the specimen was changed by adjusting the temperature of the carbon resistance furnace. The sensitivity of the IR-detector was such that measurements could be obtained at specimen temperatures of 200°C or higher. The thermocouple permitted measurements down to room temperature. The laser-flash method is particularly suitable for measurements of the thermal diffusivity for two reasons. First, the technique requires a small specimen of convenient shape. Secondly, the measurement of

---

+ Model K-1, Korad Co., Santa Monica, California
** Barnes Model IT-7B, Barnes Engineering, Stamford, Connecticut
§§ CC-Cement, Omega, Engineering, Stamford, Connecticut
++ Model 1201A, Hewlett-Packard, Palo Alto, California

the thermal diffusivity involves a small temperature increase of the specimen (only $\simeq 1^{o}C$) which is important for materials exhibiting heat transfer properties strongly dependent on temperature. In the manner described above, the thermal diffusivity was measured as a function of temperature during heating and cooling of the specimen to establish the existence of any hysteresis effect. For some specimens, these experiments were repeated on subsequent days to determine the reproducibility of the hysteresis curves and the existence of a fatigue effect. Initial experiments showed that the laser radiation introduced microcracking at specimen temperatures in excess of about $850^{o}C$. As a result, the upper specimen temperature was limited to the range of $750^{o}C$ to $800^{o}C$.

III. Results and Discussion

For the iron titanate, the microstructures and data for thermal diffusivity are shown in Figures 1 and 2. Information on the various annealing treatments and the resulting average grain sizes are included in Figure 2. The hot-pressed material without any annealing had a uniform grain size distribution with an average grain size of approximately one μm. Figure 2 clearly shows that annealing encouraged considerable grain growth, which appears to be of the discontinuous type in view of the clearly evident bi-modal grain size distribution. Grain growth appeared to occur by decreasing the fraction of small grains with increasing time of anneal. Particularly in the large-grained annealed specimens, microcracks are clearly evident. Microcracking appeared to have occurred primarily in an intergranular mode. Unfortunately, a quantitative measure of the number of cracks per unit volume, the crack size, and the geometry could not be obtained.

The thermal diffusivity of the hot-pressed material, shown in Figure 2a, exhibits a temperature dependence typical of a dielectric material in which heat transport occurs primarily by lattice conduction, i.e., phonon transport. On heating and cooling, no evidence of a hysteresis effect is found, which implies that in this fine-grained material little, if any, microcracking occurred.

In contrast, the thermal diffusivity of the annealed microcracked specimens shown in Figures 2a to 2c shows a markedly different behavior. A comparison of the numerical values for the hot-pressed and annealed specimens suggests that microcracking can lower the thermal diffusivity by as much as a factor of three. Since microcracking is expected to have only a minor effect, if any, on the density and the specific heat, the

large decrease in thermal diffusivity must be attributed primarily to the effect of microcracking on thermal conductivity. As a result, microcracking appears to be a very effective method of improving the thermal insulating properties of ceramic materials. Even if a gas phase were present within the microcracks, little or no increase in thermal conductivity or diffusivity is expected since the thermal conductivity of gases [17] such as air nitrogen is some three orders of magnitude below the value of the non-microcracked material.

A strong hysteresis effect is observed in the temperature dependence of the annealed samples as indicated in Figures 2a, 2b, and 2c. This evidence for hysteresis is in general agreement with similar observations for strength and elastic behavior referred to earlier. On the heating portion of the hysteresis curve, the thermal diffusivity shows an increase with increasing temperature. This positive temperature dependence is the result of a combination of effects. Clearly, a decrease in the iron titanate's thermal diffusivity is expected, as shown in Figure 2a. Since the degree of microcracking (in terms of crack size, crack density, etc.) is expected to be proportional to the degree of cooling below the annealing temperature, crack closure is expected on reheating. This will lead to a strong positive temperature dependence of the thermal diffusivity. A further positive temperature dependence is expected from an increased contribution of heat transfer by radiation across the cracks. The negative temperature dependence of the thermal diffusivity at the initial part of the heating curve suggests that, over this temperature range, the contribution to the temperature dependence due to crack closure or radiative heat transfer is smaller than the effect of phonon-collision. The converse is true at the higher temperatures of the heating part of the hysteresis

curve. However, in comparison to radiation over the total temperature range involved, crack closure is expected to be the most important factor in view of the hysteresis in mechanical behavior for these types of materials. Of course this hysteresis is independent of any radiation heat transfer across the cracks. A final mechanism for the positive temperature dependence of the thermal diffusivity is crack healing by diffusional processes at the higher temperatures. Due to crack healing, at least in part, during cooling, the thermal diffusivity does not return along the original heating curve. However, this observation also may be related to frictional effects, particularly for microcracks formed in shear so that the displacement between the opposing crack surfaces cannot occur in a linear manner with the degree of cooling.

The increasing time of anneal leads to no major change in the thermal diffusivity after the first 4-hour anneal. Nevertheless, a slight further decrease in thermal diffusivity with annealing time may be noted. This is to be expected when the effect of grain size on the degree of microcraking is considered. A further grain size effect may be noted on the cooling part of the hysteresis curve, which shows that the thermal diffusivity (to a first approximation) remains independent of temperature. Then a rather sharp change in temperature dependence occurs at a given temperature. This temperature for the 32-and 16-hour anneals corresponds to approximately $550^{o}C$ and $400^{o}C$, respectively. For the 4-hour anneal, this temperature appears to be below $200^{o}C$. This effect is in accordance with the previously noted relationships between degree of microcracking and grain size. For the larger grain sizes and after crack healing has occurred, the degree of cooling required to cause new microcracking is observed to be less than for fine-grained specimens.

As shown in Figures 2b and 2d, the hysteresis curves during succesive cycles do not follow the same path. This suggests that the thermal cycling introduces a permanent change in the microcrack morphology. Such a change in the hysteresis curves is particularly noticeable for the sample annealed for a 4-hour period. The area within the hysteresis curve for this sample becomes smaller on successive cycles so that cracks tend to partially heal or close during successive thermal cycling, thereby increasing the total amount of phonon transport. Since the data reported in Figure 2 were obtained with the IR-detector, no general statement can be made about the nature of hysteresis curve closure at temperatures below 200°C. A simple experiment using a thermocouple, however, indicated that hysteresis curves take on the shape of a flat figure eight similar to the one observed for magnesium dititanate with the cross-over point near 100°C and a thermal diffusivity value at the end of the cycle near the value at the beginning of the cycle.

Figure 3 shows the scanning electron micrographs of the hot-pressed and annealed magnesium dititanate specimens. Grain growth in the magnesium dititanate (as with iron titanate) appeared to be of the discontinuous type, resulting in a bimodal grain size distribution for the immediate annealing times. Microcracking appeared to occur primarily in an intergranular mode, although occasionally intragranular microcracking also could be observed. Microcracking was very apparent in the coarse-grained material, but it was not observed with any degree of certainity in the fine-grained material. Average grain size after 0, 3, 27, and 60 hours of annealing at 1200°C were approximately 1.0, 4.5, 25, and 70μm, respectively.

Experimental data for the thermal diffusivity, measured using the thermocouple, are shown in Figure 4. Again, comparing data for the thermal

diffusivity following various annealing treatments, microcracking can cause a significant decrease in thermal diffusivity. This is in agreement with data obtained for iron titanate. Again, these observations must be attributed primarily to the effect of the microcracking on the thermal conductivity. However, the thermal diffusivity of magnesium dititanate shows some fundamental differences in comparison to that of iron titanate. For the hot-pressed material, the temperature dependence of thermal diffusivity on the heating part of the curve is as expected for a non-microcracked material. It is similar to that of the non-microcracked, fine-grain iron titanate shown in Figure 2a. However, data for the cooling part of the thermal cycle fall below the corresponding values for the heating part of the curve. This results in a clockwise hysteresis curve which contrasts with the counter-clockwise hysteresis observed for microcracked iron titanate. It also should be noted that on return to room temperature, the hysteresis curve is not closed. This suggests a permanent change in the material. This behavior is consistent with the effect expected if new microcracks were formed as the result of thermal cycling, or if existing microcracks grew in size under the influence of the thermal stresses as the result of fatigue. For hot-pressed magnesium dititanate, the formation of new cracks during the cooling part of the thermal cycle appears to be the most likely mechanism. If this explanation is correct, it must be concluded that a given microcrack configuration (in terms of the crack density, geometry or orientation and degree of cooling) is not necessarily an equilibrium configuration. As a result, the properties of microcracked materials are expected to be a function of past thermal history. The validity of this conclusion is demonstrated also by literature

data covering thermal cycling's on strength and Young's modulus for magnesium dititanate and other microcracked materials.

New crack formation during thermal cycling is thought to be responsible for the figure-eight type of hysteresis curves exhibited by the annealed magnesium dititanate specimens (as shown in Figures 4b and 4d). At higher temperatures, hysteresis curves are counter-clockwise as would be expected from the effect of crack healing and closure. On cooling, however, the thermal diffusivity curve crosses the heating curve because of additional crack formation. This results in a value of thermal diffusivity lower than the original value at the beginning of the cycle. In this manner, the figure eight type of hysteresis curve is determined by the competing effects of crack healing and/or closure and the formation of new microcracks. As Figures 4b and 4c show, repeated cycling results in a decrease in the area within the hysteresis curves in a qualitatively similar manner as that observed for iron titanate.

The microstructure of aluminum titanate was quite similar in nature to the microstructures of iron titanate and magnesium dititanate. In Figure 5, the thermal diffusivity for two gran sizes is shown. Again, the figure-eight type of hysteresis curve is similar to the ones observed for magnesium dititanate and is attributable to the competing effects of crack healing and closure at the high temperature and the formation of new microcracks during cooling to the lower temperatures.

The thermal diffusivity of aluminum titanate was observed to recover during an 18-hour period between two successive thermal cycles. This suggests that some readjustment of crack morphology is possible even at relatively low temperatures in microcracked materials. This mechanism

responsible for this recovery may be identical to (or at least related to) the mechanism of creep and elastic recovery.

It is unfortunate that no quantitative measure of the crack density, crack size, and other variables describing the microcracks morphology are obtainable. Such data could have been used to predict the effect of microcracking on the thermal conductivity from theoretical solutions for the heat transfer properties of composite materials and to compare these predictions with observed results. However, even lower values of thermal diffusivity should be obtainable for more extensive microcracking in the present materials.

A final remark is in order with regard to the potential of microcracked materials for applications involving severe thermal shock. Present theory of the thermal stress fracture of ceramic materials [6,19,20] states that high thermal shock resistance requires high values of thermal conductivity. In this respect, microcracking, which causes a significant lowering of the thermal conductivity, would not appear to be beneficial in improving thermal shock resistance. However, very high strains-at-fracture in combination with a stable (non-catastrophic) mode of crack propagation far outweigh the requirement for a high thermal conductivity. This is especially so for large structures subjected to high heat flux in which thermal conductivity only plays a minor role. [6] In fact, the lower thermal conductivity of microcracked materials can be used to considerable advantage for those applications where material requirements of high thermal shock resistance in combination with good thermal insulating properties are desired.

Acknowledgments

The specimens used in this study were prepared at the Pennsylvania State University. One of the authors (J.J. Cleveland) is grateful to GTE-Sylvania for a fellowship awarded to pursue the Master's degree at Pennsylvania State University. Measurements of the thermal diffusivity, the microscopy, and the manuscript preparation were performed at Lehigh University and The Montana Energy and MHD Research and Development Insitute, Inc. as part of research programs sponsored by the Office of Naval Research under Agreements No. N00014-75-6-0761 and N00014-76-C-0884.

REFERENCES

1. E. A. Bush and F. A. Hummel, "High Temperature Mechanical Properties of Ceramic Materials - I, Magnesium Dititanate," Journal American Ceramic Society, 41 (6), p. 189 1958: "II, Beta-Eucryptite," Journal American Ceramic Society, 42 (8), p. 388, 1959.

2. J. A. Kuszyk and R. C. Bradt, "Influence of Grain Size on Effect of Thermal Expansion Anisotropy in $MgTi_2O_5$, Journal American Ceramic Society, 56 (8), p. 420, 1970.

3. W. R. Manning, O. Hunter, F. W. Calderwood, and D. W. Stacey, "Thermal Expansion of Nb_2O_5," Journal American Ceramic Society, 55 (7), pp. 342-47, 1972.

4. R. C. Rossi, "Thermal Shock-Resistant Ceramic Composites," Bulletin American Ceramic Society, 48 (7) p.736, 1969.

5. R. C. Garvie and P. S. Nicholson, "Structure and Thermo-Mechanical Properties of Partially Stabilized Zirconia in the $CaO-ZrO_2$ System," Journal American Ceramic Society, 55 (3) pp. 152-57, 1972.

6. D. P. H. Hasselman, "Unified Theory of Thermal Shock Fracture Initiation and Crack Propagation in Brittle Ceramics," Journal American Ceramic Society, 52 (11), pp. 600-04, 1969.

7. D. P. H. Hasselman, "Thermal Stress Crack Stability and Propagation in Severe Thermal Environments," Materials Science Research, Materials Science Research, Volume V, Ceramics in Severe Environments, ed. by W. W. Kriegel and Hayne Palmour III, Plenum Press, New York, pp. 89-103, 1971.

8. W. R. Buessum, "Internal Ruptures and Recombinations in Anisotropic Ceramic Materials," Mechanical Properties of Engineering Ceramics, ed. by W. W. Kriegel and H. Palmour III, Interscience Publications Incorporated, New York, pp. 127-48, 1961.

9. W. R. Buessum and F. F. Lange, "Residual Stresses in Anisotropic Ceramics," Interceramics, 15 (3), p. 299, 1966.

10. R. McPherson, "Intercrystalline Thermal Stresses in Polycrystalline Rutile," Journal American Ceramic Society, 3 (2), p. 43, 1967.

11. D. P. H. Hasselman, "On the Voight and Reuss Modulus of Polycrystalline Solids with Microcracks," Journal American Ceramic Society, 53 (3), p. 170, 1970.

12. R. W. Davidge and T. J. Tappin, "Strength of a Two Phase Ceramic-Glass Material," Journal Material Science, 3 (6), p. 692, 1968.

13. J. Selsing, "Internal Stresses in Ceramics," Journal American Ceramic Society, 44 (8), p. 419, 1961.

14. R. R. Tummula and A. L. Frieberg, "Residual Stresses in Glass-Crystal Composites," Journal Material Science, 6, p. 1421, 1971.

15. J. R. Tinklepaugh, "Metal Reinforcement and Cladding of Cermets and Ceramics," Cermets, ed. by J. R. Tinklepaugh and W. B. Crandall, Reinhold Publishing, New York, pp. 170-80, 1960.

16. W. J. Parker, R. J. Jenkins, C. P. Butler, and G. L. Abbott, "Flash Method of Determining Thermal Diffusivity, Heat Capacity, and Thermal Conductivity," Journal Applied Physics, 32 (9), pp. 1079-81, 1961.

17. E. R. G. Eckert and R. M. Drake, Jr., Heat and Mass Transfer, McGraw-Hill, New York, 1959.

18. D. P. H. Hasselman, "Crack Growth and Creep in Brittle Ceramics," Journal American Ceramic Society, 42 (9), pp. 517-18, 1969.

19. W. D. Kingery, "Factors Affecting Thermal Stress Resistance of Ceramic Materials," Journal American Ceramic Society, 38 (1) pp. 3-15, 1955.

20. D. P. H. Hasselman, Thermal Stress Resistance Parameters for Brittle Refractory Ceramics: A Compendium," Bulletin American Ceramic Society, 49 (12), 1933-37, 1970.

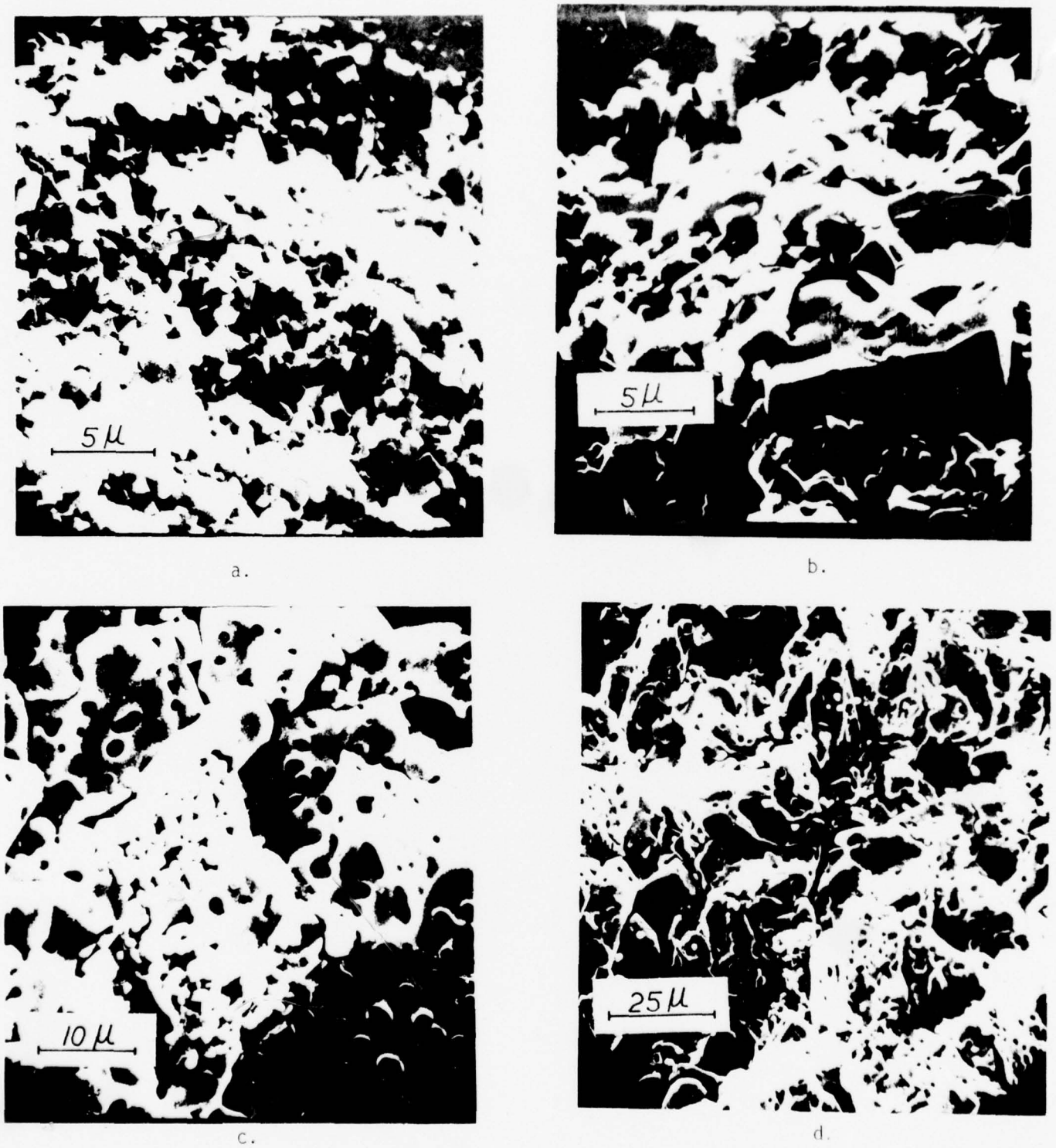

Fig. 1. Microstructures of Fe_2TiO_5; a. As hot-pressed; and annealed at 1000°C for b. 4 hrs; c. 16 hrs, and d. 32 hrs.

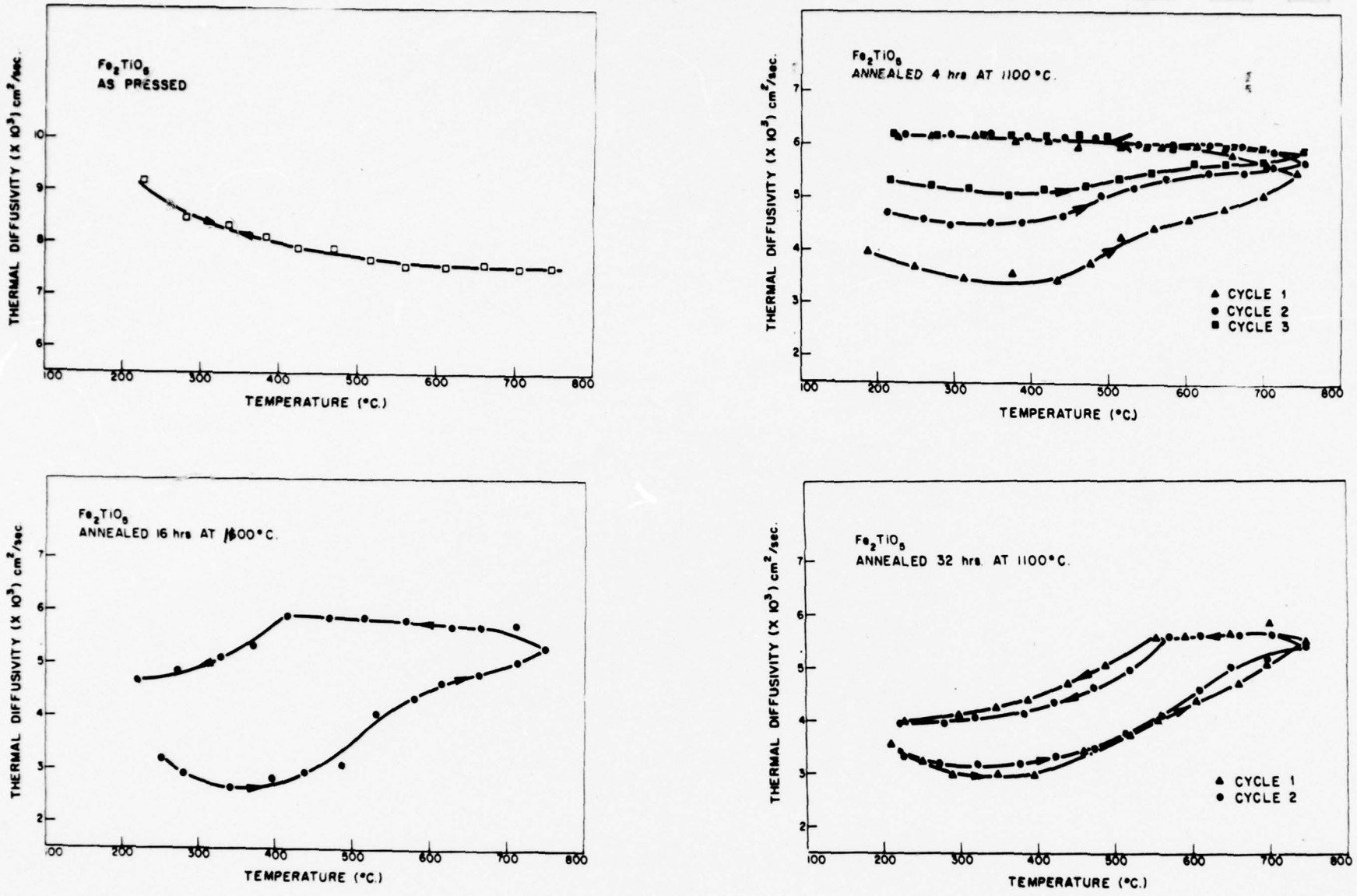

Fig. 2 Thermal diffusivity of Fe_2TiO_5 for various annealing treatments.

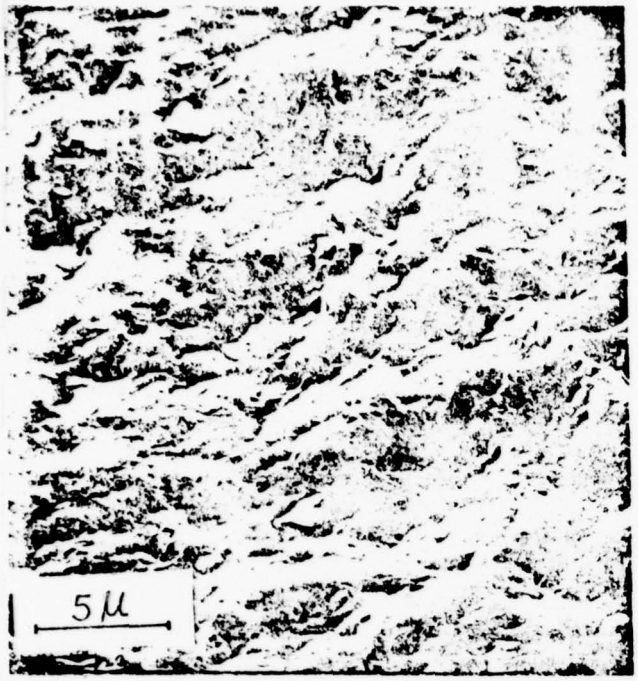

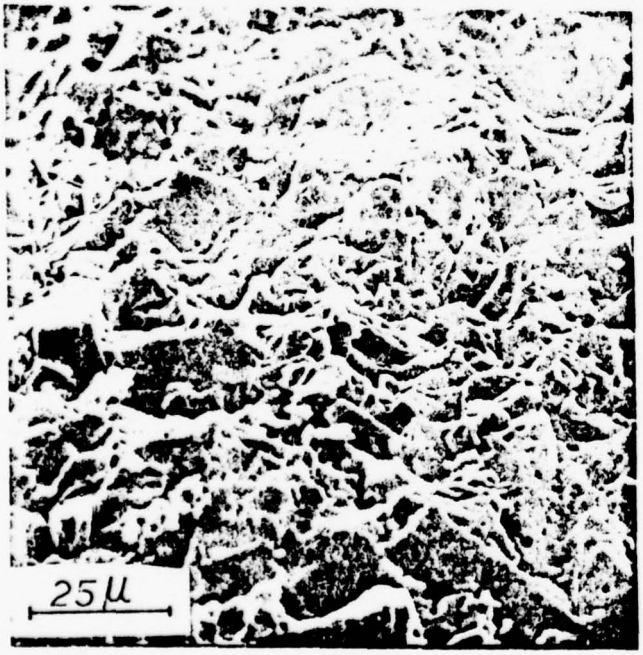

Fig. 3. Microstructures of $MgTi_2O_5$
a. As hot-pressed; and annealed at 1200°C for
b. 3 hrs; c. 27 hrs, and d. for 32 hrs.

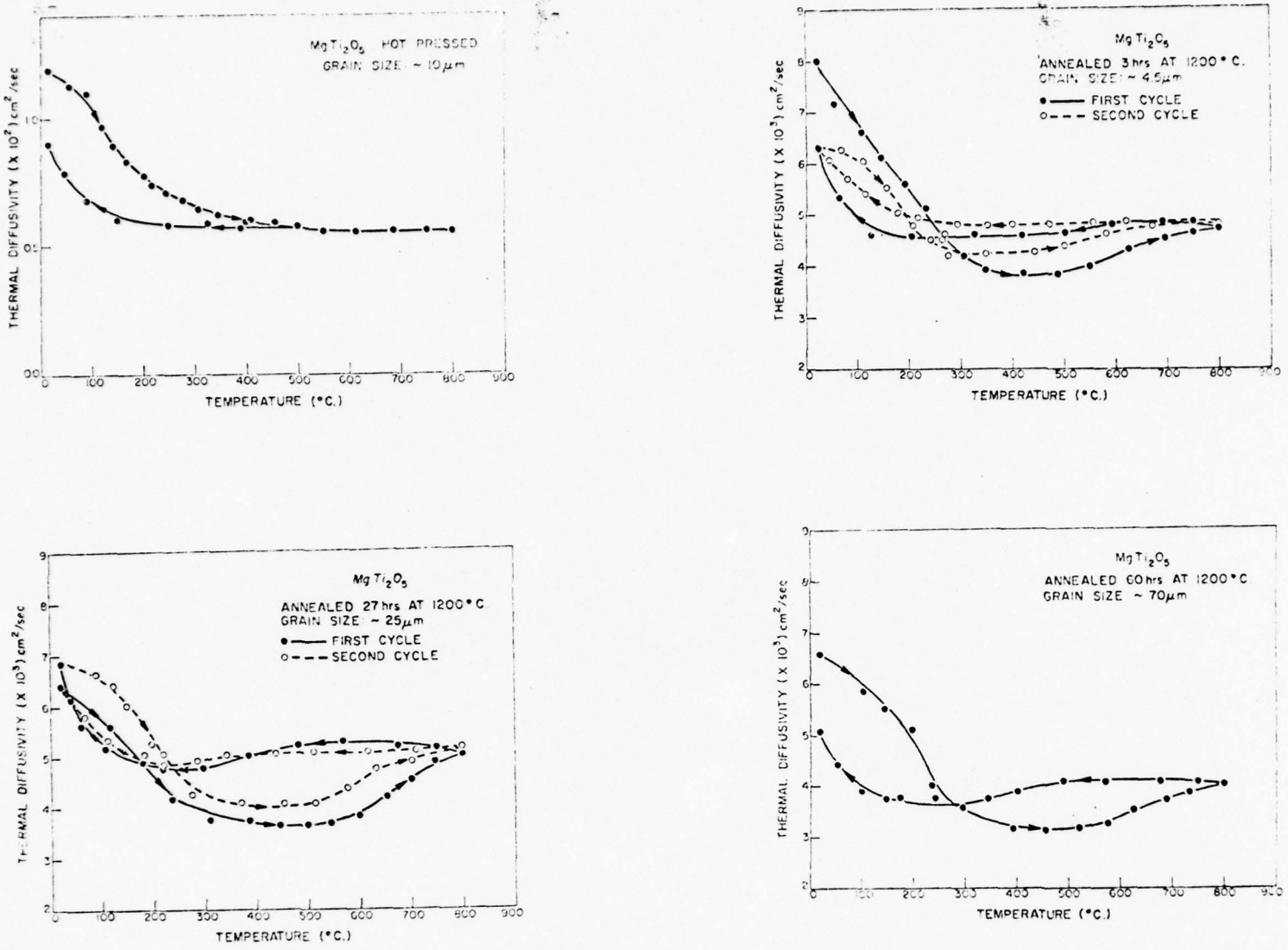

Fig. 4. Thermal diffusivity of $MgTiO_5$ for various annealing treatments.

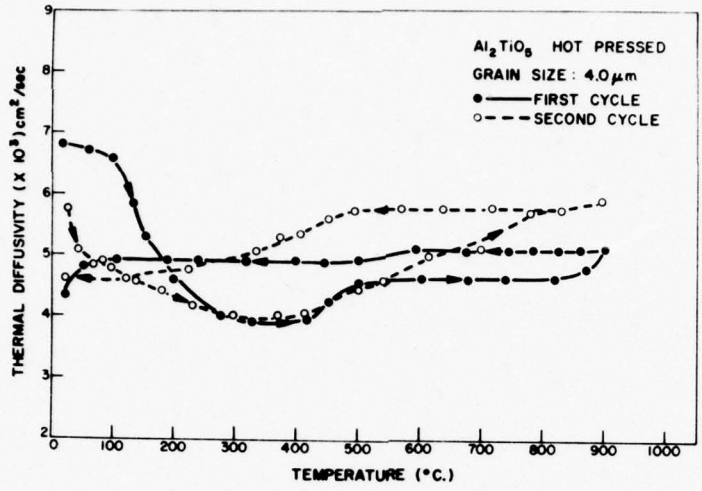

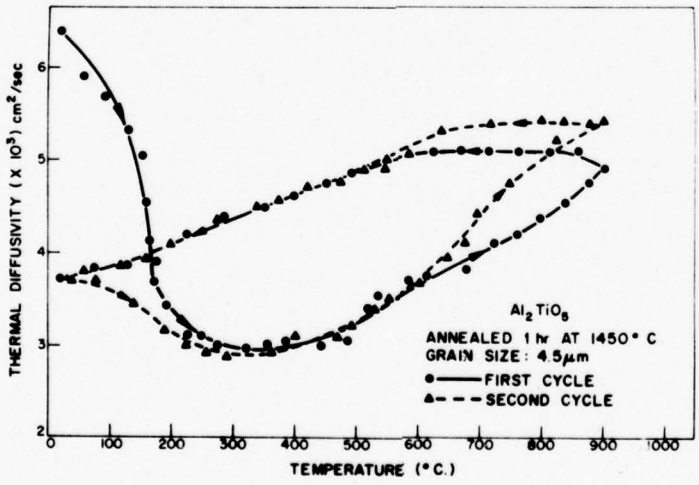

Fig. 5. Thermal diffusivity of Al_2TiO_5 for two thermal treatments.

APPENDIX B

THERMAL DIFFUSIVITY AND CONDUCTIVITY OF A FIBROUS ALUMINA

THERMAL DIFFUSIVITY AND THERMAL CONDUCTIVITY OF A FIBROUS ALUMINA

by

H. J. Siebeneck,* R. A. Penty,+ D. P. H. Hasselman,§ and G. E. Youngblood§

Engineering Note
Submitted to
Bulletin of American Ceramic Society

* University of Maryland, University Park, MD
+ Fiber Materials Inc., Biddeford, ME
§ The Montana MHD Research and Development Institute, Inc., Butte, MT

THERMAL DIFFUSIVITY AND THERMAL CONDUCTIVITY OF A FIBROUS ALUMINA

by

H. J. Siebeneck,* R. A. Penty,+ D. P. H. Hasselman,§ and G. E. Youngblood§

Porous materials, generally, are very effective thermal insulators. The relative effect of porosity on the thermal conductivity and thermal diffusivity of ceramic materials has been the subject of a number of investigations. [1-6] The present note reports data for the thermal conductivity and diffusivity of a fibrous alumina.

Samples with a range of low densities produced by hot-pressing a fibrous alumina were obtained from a commercial source.** The alumina contained approximately 10 wt. percent SiO_2. Scanning electron micrographs of samples with densities of 3.50, 2.53, 1.41, and 0.60 gm/cc are shown in Figures 1a, 1b, 1c, and 1d, respectively. Figure 1a represents the microstructure of the fully dense material. Figure 1b shows areas of open-porosity, low density fibrous material sandwiched between dense plates oriented perpendicular to the hot-pressing direction. Figure 1c and 1d show the preferred alignment of fibers perpendicular to the pressing direction in the lower density materials.

The thermal diffusivity of the four materials was measured by the laser-flash technique [7] in a nitrogen atmosphere using equipment described in detail elsewhere. [8] The direction of heat flow was parallel to the hot-pressing direction during these measurements. Because of difficulties encountered in specimen fabrication, measurement of the thermal diffusivity

---

* University of Maryland, University Park, MD
+ Fiber Materials Inc., Biddeford, ME
§ The Montana Energy and MHD Research and Development Institute, Inc., Butte, MT
** Fiber Materials Inc., Biddeford, ME

of samples with lower density was precluded. Assuming that the specific heat capacity of the fibrous alumina was similar to that reported [9] for pure alumina, the thermal conductivity (K) was calculated from

$$K = \alpha(T).\ \rho(T).C_p(T) \qquad (1)$$

where $\alpha(T)$ is the thermal diffusivity, $\rho(T)$ is the density, and $C_p(T)$ is the specific heat capacity at constant pressure and all the terms are functions of temperature.

Figure 2 shows the experimental data for the thermal diffusivity of the four samples of fibrous alumina over the temperature range of approximately 200°C to 1000°C. The calculated behavior of the thermal conductivity is shown in Figure 3. The negative slope of the temperature dependence of the hot-pressed sample is typical for high-density dielectric materials in which heat transfer occurs primarily by lattice conductivity. The positive temperature dependence of the thermal conductivity of the most porous samples suggests that radiation and gas conduction across the pores between the fibers provide a significant contribution to the heat transfer in these samples. [10] Exact quantitative calculations of the relative contribution of conduction through the solid, radiation, and gas conduction across the pores to the total thermal conductivity are expected to be difficult due to the complexity of the fibrous structure. However, as indicated by the results of Sparrow and Cur, [11] the contribution of gas conduction would be expected to exceed that of radiation in this temperature range.

The present results can be compared with those obtained for other non-fibrous porous materials. Taking the thermal conductivity of the non-porous, hot-pressed material as unity, Figure 4 shows the relative thermal conductivity at 200, 400, 600, and 800°C as a function of pore volume fraction. The present

data gives a reasonable fit to the semi-empirical equation based on expressions of Maxwell - Eucken, [12] Fricke, [13] and Biancheria [14] and which can be written in the general form

$$\frac{K}{K_o} = \frac{1 - P}{1 + \beta P} \qquad (2)$$

where K and K_o are the thermal conductivities of the porous and non-porous material, respectively, P is the fractional porosity, and β is a parameter which depends upon pore shape as well as the fractional porosity.

Equation (2) is included in Figure 4 for various values of β. The best fit is obtained for the data at 200°C with $\beta \simeq 4$. With increasing temperature β decreases as expected from the increased heat transfer by radiation and gaseous conduction across the pores. Such a decrease of β with temperature would require a theoretical analysis similar to Marino's [4] analysis for elliptical pores where it is shown that β is a general function of temperature as well as pore fraction and shape. Also, as indicated by Figure 4, β increases with increasing pore content, which in this case is probably attributable to the decrease in content of solid-plate material with increasing porosity. As can be determined from the data for thermal conductivity for some of the ceramic materials at temperatures comparable to 200°C reviewed by Rhee*, $\beta \simeq 0.4$ for the porous uranium dioxide data of Ross, [17] $\beta = 0$ for the isometric pores in alumina data of Francl and Kingery, [2] and $\beta \simeq 2$ for the anisometric pores in hot-pressed alumina data of McClelland and Petersen. [3] In addition, theory [18] shows that for isolated spherical pores of zero conductivity $\beta = \frac{1}{2}$. Comparison of these

* The expression of Aivazov and Domashnev (ref. 15), found by Rhee (ref. 16) to apply to a wide variety of ceramic materials with non-fibrous pore structures, does not give an acceptable explanation for the dependence of the relative conductivity on porosity fraction for our data.

values with the value of $\beta \simeq 4$ for the present study suggests that porosity found in a fibrous material is more effective in lowering the thermal conductivity than more isometric pores found in sintered materials.

Acknowledgment

This study was carried out as part of a larger research program on the thermal conductivity and diffusivity of engineering ceramics supported by the Office of Naval Research under agreements No. N00014-75-C-0760 and No. N00014-76-C-0884. The authors are indebted to Mr. Paul Urick for preparing the fully dense hot-pressed material.

REFERENCES

1. A. L. Loeb, "Thermal Conductivity: VII - A Theory of Thermal Conductivity of Porous Materials," Journal American Ceramic Society, 37, p. 96, 1954.

2. J. Francl and W. D. Kingery, "Thermal Conductivity: IX, Experimental Investigation of Effect of Porosity on Thermal Conductivity," Journal American Ceramic Society, 37, p. 99, 1954.

3. J. D. McClelland and L. O. Petersen, "The Effect of Porosity on the Thermal Conductivity of Alumina," Technical Report NAA-6473, Atomics International, Canoga Park, California, October 30, 1961.

4. G. P. Marion, "The Porosity Correction Factor for the Thermal Conductivity of Ceramic Fuels," Journal Nuclear Material, 38, p. 178, 1971.

5. P. Wagner, J. A. O'Rourke, and P. E. Armstrong, "Porosity Effects in Polycrystalline Graphite," Journal American Ceramic Society, 55, p. 214, 1972.

6. W. Woodside and J. H. Messmer, "Thermal Conductivity of Porous Media II: Consolidated Rocks," Journal Applied Physics, 32, p. 1699, 1961.

7. W. J. Parker, R. J. Jenkins, C. P. Butler, and G. L. Abbott, "Flash Method of Determining Thermal Diffusivity, Heat Capacity and Thermal Conductivity," Journal Applied Physics, 32, p. 1697, 1961.

8. J. E. Matta and D. P. H. Hasselman, "The Thermal Diffusivity of Al_2O_3 - Cr_2O_3 Solid Solutions," Journal American Ceramic Society, 58, p. 458, 1975.

9. V. S. Touloukian, R. W. Powell, C. Y. Ho, and P. G. Klemens, Specific Heat - Nonmetallic Solids, Volume 5 of Thermophysical Properties of Matter Series, IFI/Plenum, New York, p. 35, 1970.

10. W. D. Kingery, H. K. Bowen, and D. R. Uhlmann, Introduction to Ceramics, 2nd Ed., John Wiley and Sons, New York, p. 639, 1976.

11. E. M. Sparrow and N. Cur, "Characteristics of Hollow Glass Microspheres as an Insulating Material and an Opacifier," Journal of Heat Transfer, P. 232, May 1976.

12a. J. C. Maxwell, A Treatise on Electricity and Magnetism, 1, 3rd Ed., Oxford: Oxford U. Press, p. 440, 1904.

12b. A. Eucken, "Thermal Conductivity of Ceramic Refractory Materials," Forsch, Gebitet Ingenieur B-3, March-April 1932.

13. Hugo Fricke, "The Electrical Conductivity of a Suspension of Homogeneous Spheroids," Physical Review, 24, p. 575, 1924.

14. A. Biancheria, "The Effect of Porosity on Thermal Conductivity of Ceramic Bodies," Transactions American Nuclear Society, 9, p. 15, 1966.

15. M. I. Aivazov and I. A. Domashnev, "Influence of Porosity on the Conductivity of Hot-Pressed Titanium Nitride Specimens," Poroshkovya Met. 8, p. 51, 1968.

16. S. K. Rhee, "Porosity - Thermal Conductivity Correlations for Ceramic Materials," Materials Science and Engineering, 20. p. 89,1975.

17. A. M. Ross, "The Dependence of the Thermal Conductivity of Uranium Dioxide on Density, Microstructures, Stoichiometry, and Thermal-Neutron Irradiation, 'Atomic Energy Canada, Ltd. CRFD - 187, September 1960.

18. J. B. Austin, in Symposium on Thermal Insulating Materials, American Society Testing Materials, Philadelphia, Pennsylvania, p.3, 1939.

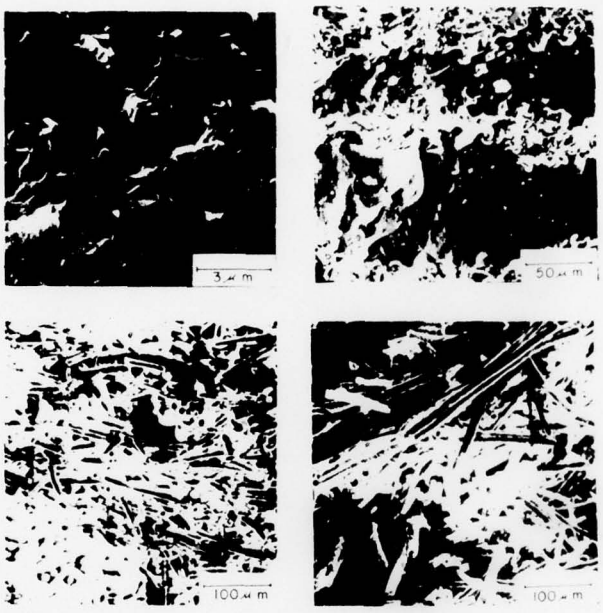

Fig. 1 Scanning electron micrographs of fibrous alumina: (a) hot-pressed, 3.50 gm/cc, (b) 2.53 gm/cc, (c) 1.41 gm/cc, and (d) 0.60 gm/cc

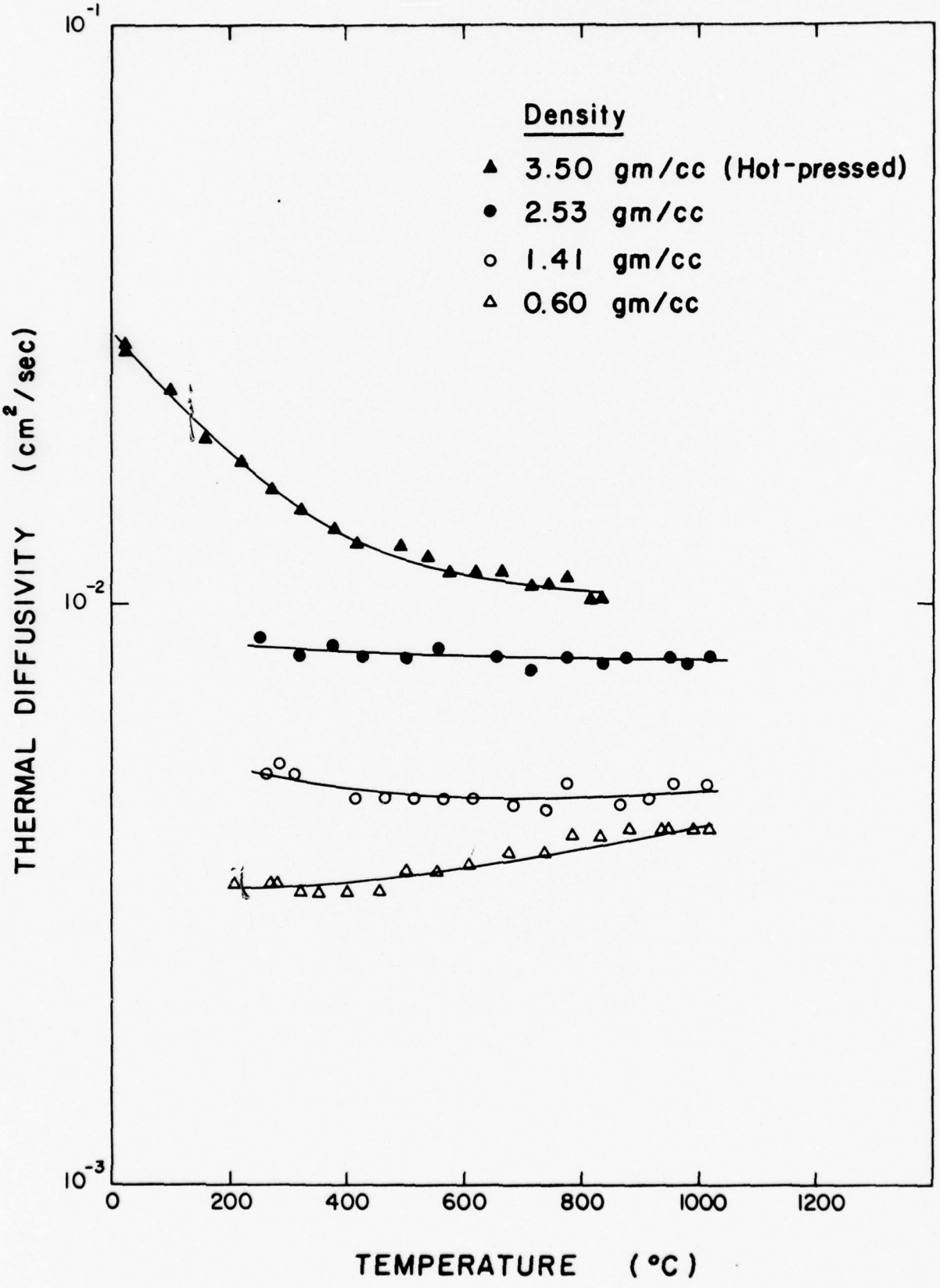

Fig. 2 Thermal diffusivity of fibrous alumina as a function of temperature and density.

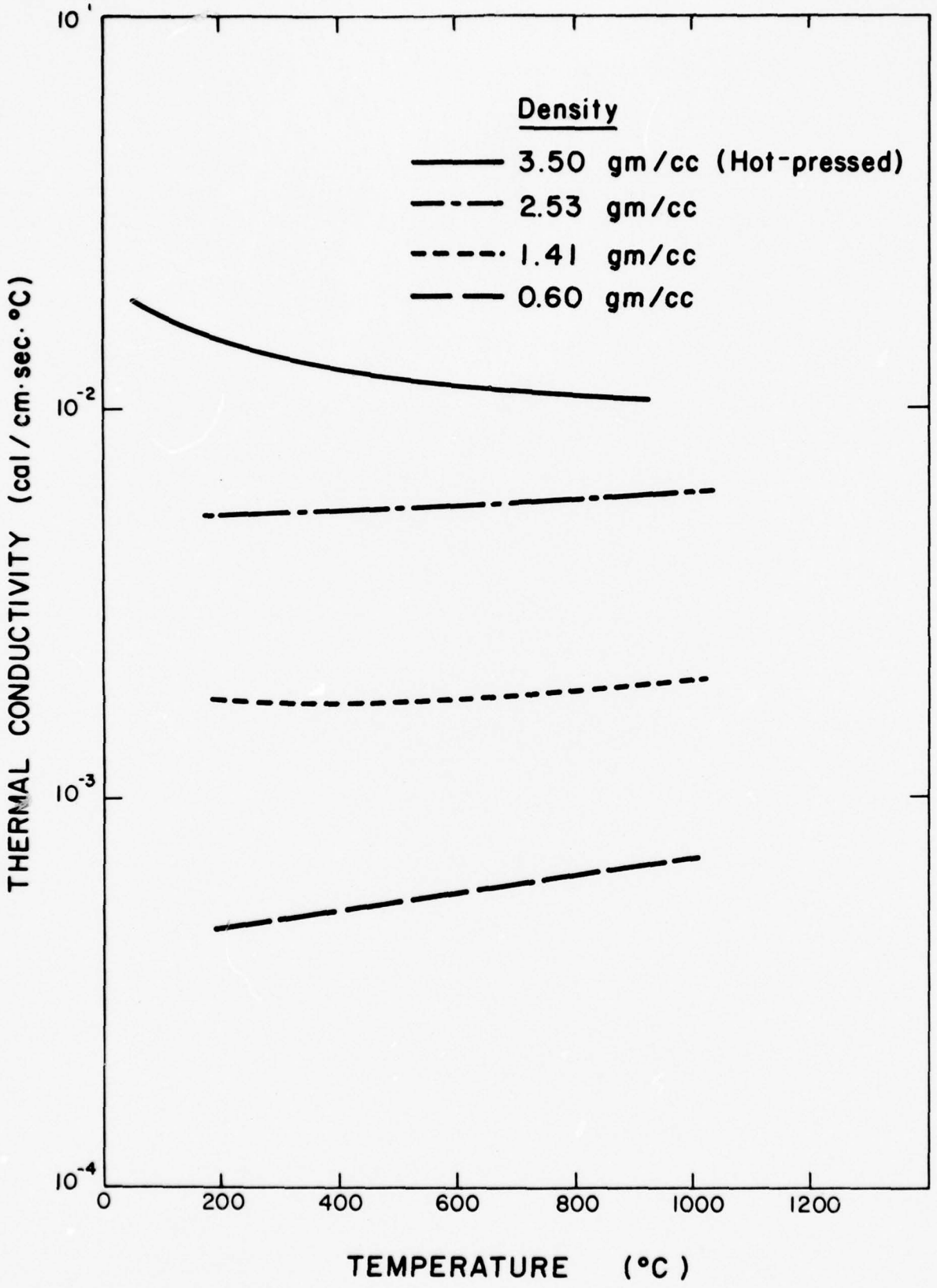

Fig. 3 Calculated thermal conductivity of fibrous alumina as a function of temperature and density.

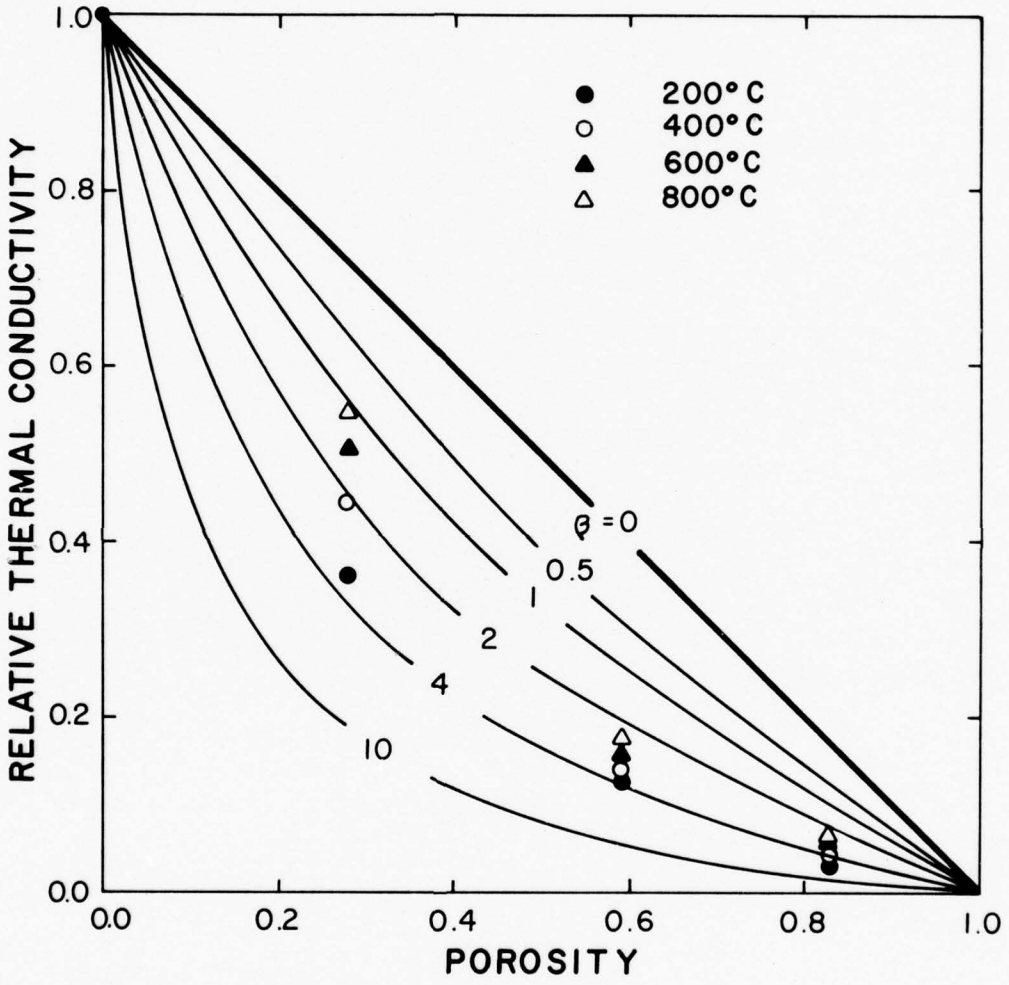

Fig. 4 Relative thermal conductivity of fibrous alumina as a function of pore volume fraction and temperature.

APPENDIX C

THERMAL DIFFUSIVITY / CONDUCTIVITY OF ALUMINA WITH A ZIRCONIA DISPERSED PHASE

THERMAL DIFFUSIVITY/CONDUCTIVITY OF ALUMINA WITH A ZIRCONIA DISPERSED PHASE

by

D. Greve*
N. Claussen+
D. P. H. Hasselman§
G. E. Youngblood§

* Lehigh University, Bethlehem, PA
\+ Max-Planck-Institut Für Metallforschung, Institut Für Werkstoffwissenschaften, Stuttgart 80, West Germany
§ The Montana Energy and MHD Research and Development Institute, Inc., Butte, MT

THERMAL DIFFUSIVITY/CONDUCTIVITY OF ALUMINA WITH A ZIRCONIA DISPERSED PHASE

D. Greve,* N. Claussen,+ D. P. H. Hasselman,§ and G. E. Youngblood§

Microcracking in brittle ceramic materials can have a pronounced effect on physical properties. Microcracking, through an enhancement of the strain-at-fracture, can lead to a major increase in thermal stress resistance. [1,2] Increases in the fracture toughness, [3] work-of-fracture, [4] and a generally stable mode of crack propagation [5] in microcracked materials also promote thermal stress damage resistance [6] in combination with excellent thermal insulating properties. [7]

In non-cubic polycrystalline materials microcracking can result from the thermal expansion anisotropy of the individual grains during thermal cycling. This class of materials will generally exhibit considerable hysteresis in strength, [1,2] elastic properties, [1,2] and as reported recently in thermal diffusivity [7,8] as well. This hysteresis is thought to be due to crack closure and healing at higher temperatures and/or frictional effects in microcracks formed by shear deformation. Microcracking also can occur in composites with differences in the thermal expansion coefficients of the individual components, or as the result of crystalline phase transformation accompanied by a volume change. [9,10]

---

* Lehigh University, Bethlehem, PA
+ Max-Planck-Institut Für Metallforschung, Institut Für Werkstoffwissenschaften, Stuttgart 80, West Germany
§ The Montana Energy and MHD Research and Development Institute, Inc., Butte, MT

The present note reports the effect of microcracking, resulting from such a phase transformation, on the thermal diffusivity and its hysteresis for a composite system consisting of a dispersed phase of unstabilized zirconia in an alumina matrix. On cooling from the sintering temperature, the zirconia particles expand during the tetragonal to monoclinic phase transformation, tensile stresses are produced in the surrounding alumina matrix, and a high density of microcracks are formed in the alumina.

Following procedures described previously, [3] samples of pure alumina‡ and alumina with 16 volume percent unstabilized zirconia** were fabricated by hot-pressing. For these samples the fracture toughness K_{1c} was found to be 5.06 ± 0.32 and 7.14 ± 0.19 $MN/m^{3/2}$, respectively. The significant increase in fracture toughness is indicative of the presence of microcracks in the alumina with 16 percent zirconia. TEM micrographs, presented previously, [3,11] also revealed the existence of microcracks. Dilatometry showed that the phase transformation, presumably the formation stage for most of the microcracks, occurs in the 600 to 800°C temperature range for this composite material. [11]

The thermal diffusivity was measured on discs (≃ 0.5 inches in diameter and 0.1 inches thick) by the laser-flash technique [12] using equipment described in detail earlier. [13] The transient temperature was monitored with a chromel-alumel thermocouple attached to the back face of the specimen with ceramic cement.X Measurements were made on heating and cooling between room

---

‡ 99.5% pure, Alcoa A16, Aluminum Co. of America, Pittsburgh, PA
** 1.25μm Fisher subsieve size, No. 8914, E. Merck, Darmstadt, West Germany
X CC-cement, Omega Engineering, Stamford, CT

temperature and 800°C. Densities were measured by the liquid immersion technique. The pure alum na and the alumina/16 percent zirconia composite had densities of 3.93 and 4.17 gm/cc, respectively.

The experimental thermal diffusivity data are shown in Figure 1. It is clearly evident that the presence of the zirconia particles in the alumina matrix lowers the thermal diffusivity approximately by a factor of two.

The thermal conductivity (K) was calculated from $K = \alpha\rho c$ where α is the experimentally determined thermal diffusivity, ρ is the measured density, and c is the specific heat capacity. The heat capacities for pure alumina and zirconia were obtained from Touloukian, et al [14] and used to compute the heat capacity for the alumina/zirconia composite. Since the densities of the samples were near theoretical, the calculated values of thermal conductivity were not corrected for porosity.

In Figure 2, the calculated thermal conductivity as a function of temperature is shown for each material. Since the relative decrease in specific heat approximately equals the relative increase in density when zirconia is mixed with alumina, the factor of about two decrease in the thermal diffusivity of the composite corresponds to a similar decrease in the thermal conductivity as shown by the difference between the upper and lower curves in Figure 2.

The decrease in the composite's thermal conductivity is the result of two simultaneous effects. Since the thermal conductivity of the zirconia dispersed phase is less* than the thermal conductivity of the alumina matrix,

---

* No values of thermal conductivity for "pure" monoclinic zirconia are available. Therefore a temperature independent value of 0.01 cal/gm cm °C sec for 91.6% ZrO_2 - 8.4% Al_2O_3 [15] was used in the calculation.

a decrease is expected. Assuming that the zirconia particles consist of spherical inclusions,+ the temperature dependence of the composite thermal conductivity (K_m) can be calculated from the well-known Maxwell-Eucken [16] relationship

$$K_m = K_c \left\{ \frac{1 + 2V_d \left[\frac{(1 - K_c/K_d)}{(2K_c/K_d + 1)} \right]}{1 - V_d \left[\frac{(1 - K_c/K_d)}{K_c/K_d + 1} \right]} \right\}$$

where K_c is the conductivity of the continuous matrix phase and K_d is the conductivity and V_d is the volume fraction of the spherical dispersed phase. Using our experimentally determined K_c values for alumina and handbook K_d values for zirconia*, K_m was calculated for $V_d = 0.16$ and also is shown for comparison in Figure 2. It is clear that the contribution of the lower thermal conductivity of the zirconia addition would decrease the thermal conductivity of the composite a relatively small amount compared to the total observed reduction. Most of the large decrease in the thermal conductivity must be attributed to the presence of microcracks.

Of significant importance is the observation that there was no hysteresis in the thermal diffusivity of the alumina/zirconia composite on heating and cooling below 800°C. This contrasts sharply with the observation of considerable hysteresis in Fe_2TiO_5 and $MgTi_2O_5$. [7,8] This difference in hysteresis behavior must be attributed to the difference in mechanisms responsible for the microcracking. For the titanates, in which microcracking results from thermal

---

+ Isolated and approximately spherical particles of zirconia in the alumina matrix are revealed in the TEM micrographs of reference. [3,11]

expansion anisotropy, the degree of microcracking (number, size, and separation width of the cracks) is a function of the amount of cooling from the specimen preparation temperature (strictly the temperature below which any internal stresses can no longer relax due to creep). On heating, the degree of microcracking is reduced by crack healing due to diffusional processes or other mechanisms. Crack closure or reopening during temperature cycling then gives rise to the hysteresis effect. In contrast, microcracking in the alumina/zirconia composite system occurs as the result of the phase transformation in the temperature range near the upper limit of the present observations. Below the transformation temperature, the degree of microcracking is unaffected by temperature cycling to a first approximation and crack closure is avoided. Once formed, the microcrack structure is maintained by the expanded zirconia particles. Therefore, the thermal diffusivity, which has been considerably reduced by the formation of the microcracks, no longer changes with temperature cycling.

The lack of hysteresis in the thermal diffusivity of the alumina/zirconia composite on temperature cycling below the zirconia transformation temperature also should be observed for mechanical properties, such as fracture toughness or thermal expansion. This conclusion is particularly applicable for the development of high temperature materials which permanently combine high thermal shock resistance with good thermal insulating properties during temperature cycling.

Acknowledgment

This study was carried out as part of a larger research program on the thermal conductivity and diffusivity of engineering ceramics supported by the Office of Naval Research under agreement Nos. 00014-75-C-0760 and 00014-76-C-0884.

REFERENCES

1. E. A. Bush and F. A. Hummel, "High-Temperature Mechanical Properties of Ceramic Materials: I, Magnesium Dititanate," Journal American Ceramic Society, 41, p. 189, 1958.

2. E. A. Bush and F. A. Hummel, "High-Temperature Mechanical Properties of Ceramic Materials: II, Beta-Eucryptite," Journal American Ceramic Society, 42, p. 288, 1959.

3. Nils Claussen, "Fracture Toughness of Al_2O_3 with an Unstabilized ZrO_2 Dispersed Phase," Journal American Ceramic Society, 59, p. 49, 1976.

4. J. A. Kuszyk and R. C. Bradt, "Influence of Grain Size on Effects of Thermal Expansion Anisotropy in $MgTi_2O_5$," Journal American Ceramic Society, 56, p. 420, 1970.

5. D. P. H. Hasselman, "Unified Theory of Thermal Shock Fracture Initiation and Crack Propagation in Brittle Ceramics," Journal American Ceramic Society, 52, p. 600, 1969.

6. R. C. Rossi, "Thermal-Shock-Resistant Ceramic Composites," American Ceramic Society Bulletin, 48, p. 736, 1969.

7. H. J. Siebeneck, D. P. H. Hasselman, J. J. Cleveland, and R.C. Bradt, "*Effect of Microcracking on the Thermal Diffusivity of* Fe_2TiO_5," Journal American Ceramic Society, 58, p. 241, 1976.

8. H. J. Siebeneck, J. J. Cleveland, D. P. H. Hasselman, and R.C. Bradt, "Effect of Microcracking on the Thermal Diffusivity of $MgTi_2O_5$," submitted to Journal American Ceramic Society.

9. R. C. Garvie and P. S. Nicholson, "Structure and Thermo-Mechanical Properties of Partially Stabilized Zirconia in the CaO-ZrO_2 System," Journal American Ceramic Society, 55, p. 152, 1972.

10. D. J. Green, P. S. Nicholson, and J. O. Embury, "Fracture Toughness of a Partially Stabilized ZrO_2 in the System CaO-ZrO_2," Journal American Ceramic Society, 56, p. 619, 1973.

11. Nils Clausen, Jörg Steeb, and R. F. Pabst, "Effect of Induced Microcracking on the Fracture Toughness of Ceramics," submitted to Journal American Ceramic Society.

12. W. J. Parker, R. J. Jenkins, C. P. Butler, and G. L. Abbott, "Flash Method of Determining Thermal Diffusivity, Heat Capacity, and Thermal Conductivity," Journal Applied Physics, 32, p. 1697, 1961.

13. J. E. Matta and D. P. H. Hasselman, "The Thermal Diffusivity of Al_2O_3-Cr_2O_3 Solid Solutions," Journal American Ceramic Society, 58, p. 458, 1975.

14. Y. S. Touloukian, R. W. Powell, C. Y. Ho, and P. G. Klemens, Specific Heat - Nonmetallic Solids, Volume 5 of Thermophysical Properties of Matter Series, IFI/Plenum, New York, pp. 25 and 293, 1970.

15. Y. S. Touloukian, R. W. Powell, C. Y. Ho, and P. G. Klemens, Thermal Conductivity - Nonmetallic Solids, Volume 5 of Thermophysical Properties of Matter Series, IFI/Plenum, New York, p. 441, 1970.

16. W. D. Kingery, Introduction to Ceramics, 1st. ed., John Wiley and Sons, Inc., New York, p. 501, 1960.

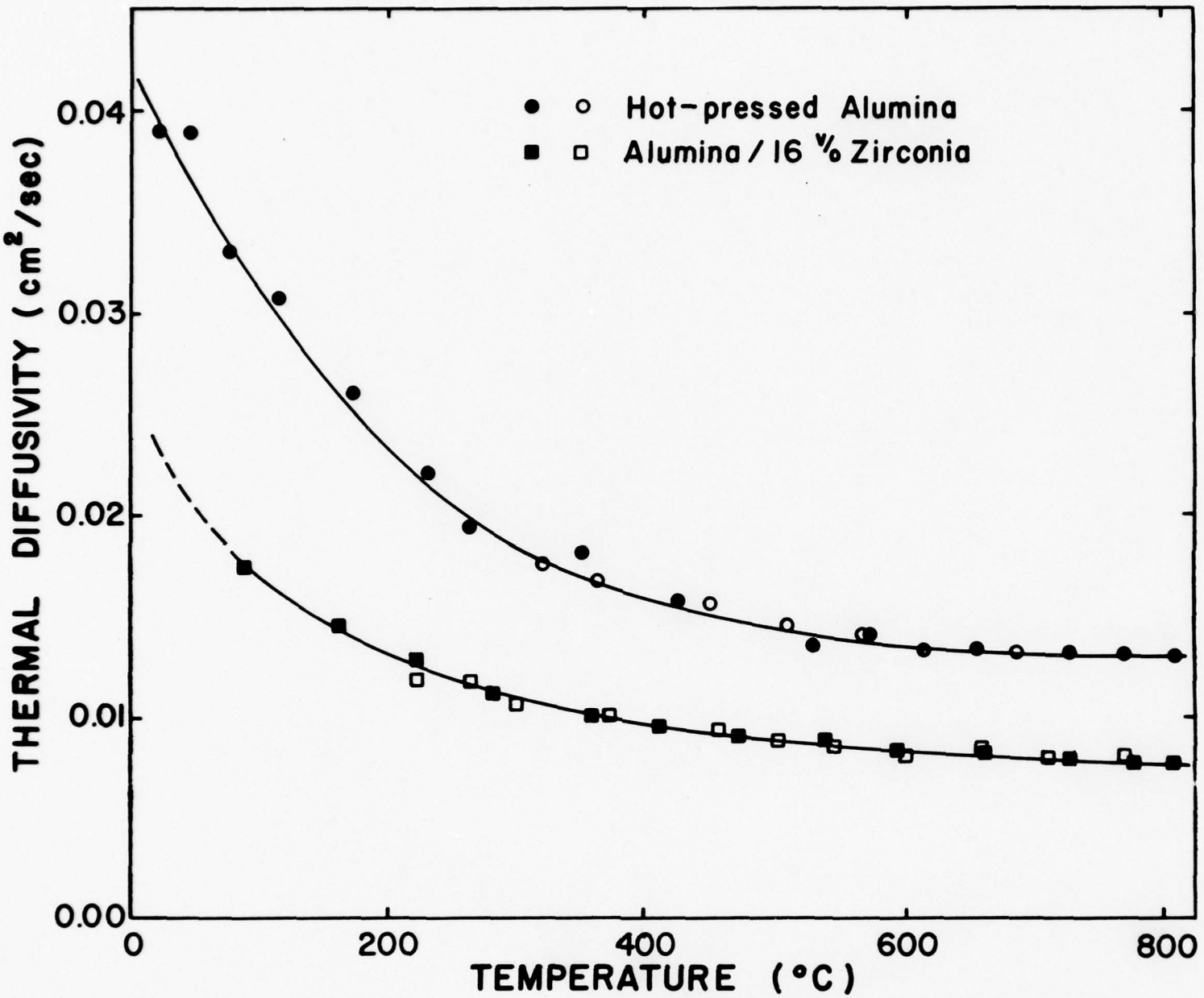

Fig. 1 Thermal Diffusivity of Hot-Pressed Alumina and a Microcracked Alumina Matrix Containing an Unstabilized Zirconia Dispersed Phase on Heating (solid symbols) and on Cooling (open symbols).

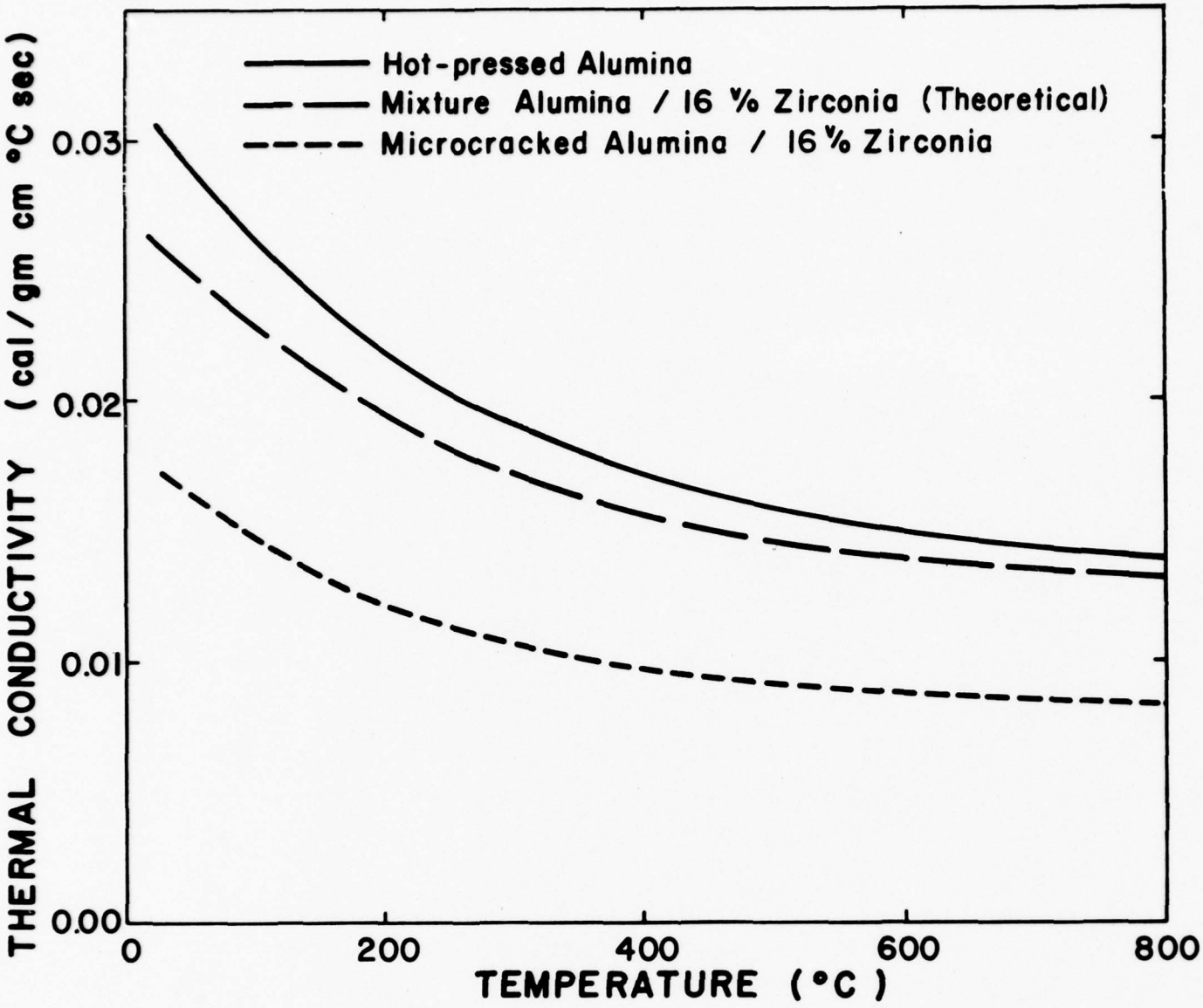

Fig. 2 Comparison of the Calculated Thermal Conductivity. Three cases: 1) Hot Pressed Alumina, 2) An Alumina with 16 percent Zirconia Dispersed Phase calculated using the theoretical relation of Maxwell-Eucken, and 3) A microcracked Alumina with 16 percent Zirconia Dispersed Phase.

APPENDIX D

EFFECT OF MICROCRACKING ON THE THERMAL DIFFUSIVITY OF POLYCRYSTALLINE ALUMINUM NIOBATE

Effect of Microcracking on the Thermal Diffusivity of Polycrystalline Aluminum Niobate

W. R. Manning*, G. E. Youngblood† and D. P. H. Hasselman*†

*Champion Spark Plug Company, Detroit, Michigan 48234

†Montana Energy and MHD Research and Development Institute, Butte, Montana 59701

*Present address: Department of Materials Engineering
Virginia Polytechnic Institute and State University
Blacksburg, Va. 24061

Effect of Microcracking on the Thermal Diffusivity of Polycrystalline Aluminum Niobate

W. R. Manning*, G. E. Youngblood† and D. P. H. Hasselman*†

*Champion Spark Plug Company, Detroit, Michigan 48234

†Montana Energy and MHD Research and Development Institute, Butte, Montana 59701

*Present address: Department of Materials Engineering
Virginia Polytechnic Institute and State University
Blacksburg, Va. 24061

Microcracks in brittle ceramic materials can have a profound effect on physical properties such as mechanical behavior and thermal properties.[1,6] In addition, on heating and cooling a significant hysteresis effect also is frequently observed. In two previous studies the effect of micro-cracking and corresponding hysteresis behavior was reported for the thermal diffusivity of iron titanate[5] and magnesium dititanate.[6] The present note reports results for the effect of micro-cracking on the thermal diffusivity of polycrystalline aluminum niobate.

Aluminum niobate ($AlNbO_4$) was prepared by the solid state reaction between powders of Al_2O_3* and Nb_2O_5**. The materials were mixed by dry-ball-milling for five hours followed by firing in air for 4 hours at 1200°C. The resulting $AlNbO_4$ powder was then dry-ballmilled an additional 5 hours and screen-granulated with 4 w/o paraffin. Two billets were prepared by cold pressing at 1.4×10^8 $N.m^{-2}$ followed by firing in air at 1350°C for periods of two hours. One of these billets was fired for an additional 24 hours at 1400°C to promote grain growth. The density for both these billets was 4.20 gm. cc^{-1}. A third billet was prepared by hot-pressing in a graphite die at 1300°C and a pressure of 2.5×10^7 $N.m^{-2}$ for 2 hours, in order to obtain a fine-grained sample with a minimum degree of micro-cracking. The density for this piece was found to be 4.31 gm. cc^{-1}.

Figure 1 shows typical SEM micrographs of fracture surfaces of the three billets. The grain size of the hot-pressed billet, determined from micrographs by the linear intercept method, was of the order of 2 μm. The billet, fired for two hours at 1350°C, had an average grain size of about 3 μm which increased

* Alcoa A-16, 99.5% purity

** Kennametal, 99.5% purity

to about 7 μm during the subsequent firing at 1400°C for 24 hours. No evidence of microcracking could be found for the hot-pressed billet. Numerous SEM micrographs indicated the presence of microcracks in the sintered samples. Unfortunately, no quantitative measure of the micro-crack density and the crack size distribution was possible. The grain size dependence of the degree of microcracking is in agreement with observation reported previously.[3,5,6]

The thermal diffusivity of the aluminum niobate was measured from room temperature to about 850°C by the laser-flash technique [7] using a specimen geometry and equipment described in detail elsewhere.[5,6] The transient temperature response of the specimen was monitored by a thermocouple attached to the specimen with ceramic cement. A total heating and cooling cycle was completed within a single day, taking approximately 12 hours.

The experimental data for the thermal diffusivity are shown in figure 2. For the fine-grained hot-pressed sample the data for heating and cooling coincide, indicative of the absence of micro-cracking.* In contrast, the two coarser-grained samples exhibit significant hysteresis, as expected from the dependence of micro-cracking on grain size.[3,5,6] The maximum decrease in thermal diffusivity of the present samples due to the micro-cracking is of the order of 40%. This decrease is somewhat less than observed for iron-titanate or magnesium dititanate, which may be attributed to the smaller range of grain size of the present samples combined with differences in the thermal expansion anisotropy. Since the specific density of the present samples is hardly, if any, affected by the micro-cracking, the observed changes in diffusivity can be attributed primarily to changes in thermal conductivity, since the micro-cracks are significant barriers to heat flow.

---

* A duplicate experiment, using an IR-detector for monitoring the transient specimen temperature, also indicated a complete absence of hysteresis for the hot-pressed specimen to temperatures as high as 1000°C.

Of interest to note is that for the coarser grained samples the thermal diffusivity on cooling exceeds the values on the heating part of the cycle. This is indicative of a permanent crack healing and/or closure at the higher temperatures without new crack formation or opening on subsequent cooling. This behavior is in contrast to the observations for iron titanate[5] and magnesium dititanate[6] which show evidence of extensive new crack formation or crack opening. For the present samples no such new crack formation exists which suggests that the crack healing/closure is permanent. In fact, a repeat heating and cooling of the two coarse-grained samples show no hysteresis; the data for thermal diffusivity coincides with the cooling curves of the first cycle in Fig. 2. This indicates that the effect of micro-cracking on physical properties appears to be a maximum after the first cooling from the firing temperature. Previously[5,6] it was suggested that such a recovery in thermal diffusivity was due to crack healing or closure or to a change in crack morphology which permitted increased heat transfer by radiation along the crack.

However, a more plausible and more fundamental explanation can be given. This explanation, as discussed by Hasselman[8] in detail, is based on the fact that crack propagation under thermal stress can occur in a stable or unstable (catastrophic) manner. For stable crack propagation the driving force for additional crack propagation equals the surface energy required for fracture surface formation. Under these conditions the crack length is always directly dependent on the degree of cooling. During unstable crack propagation, however, the elastic energy released exceeds the surface fracture energy; the excess energy is converted into kinetic energy of the propagating crack. The crack will continue to gain kinetic energy until the elastic energy released equals the fracture surface energy which is the condition at which a stable crack would be arrested. The unstable crack, however, will continue to propagate until all

the kinetic energy is transformed into fracture surface energy (neglecting other forms of energy dissipation). As a result the final crack length which results from unstable propagation is "subcritical" with a length in excess of the length which would have been formed under the same cooling conditions for stable crack propagation. For such a "subcritical" crack, closure or healing of the excess length will reduce the sum of the elastic and surface energy until the length of the stable crack configuration is reached. At the higher temperatures at which the cracks are expected to be closed or nearly so, such crack healing should occur with little, if any, material transport. Stable cracks should also heal at the higher temperatures; but these should re-open on subsequent cooling. Subcritical cracks which healed over their range of "subcriticality," however, will not re-open or re-form, resulting in a permanent recovery of the thermal diffusivity. The experimental data for the present aluminum niobate samples are consistent with the behavior expected if the original micro-cracks when formed propagated in an unstable manner. The excess length of the sub-critical crack heals or closes permanently during the subsequent re-heat for the measurement of the thermal diffusivity.

In general, the length for stable or unstable crack arrest is expected to be a function of environmental factors. If after crack healing in an inert environment the samples were held in a stress-corrosive environment, new micro-crack growth by a fatigue process may occur. Under these conditions a time-dependent change in physical properties is expected. For instance, Manning[9] observed a nearly 50% decrease in Young's modulus of Nb_2O_5 over a 24-hour period following a prior heating to high temperature.

Acknowledgment

Specimen preparation was performed by the Champion Spark Plug Company.

The thermal diffusivity was measured as part of a research program sponsored by the Office of Naval Research under agreement No. N00014-76-C-0884.

REFERENCES

1. W. R. Buessum, Mechanical Properties of Engineering Ceramics, ed. by W. W. Kriegel and H. Palmour III, Interscience Publication, Inc., New York, pp. 127-48, 1961.

2. E. A. Bush and F. A. Hummel, "High-Temperature Mechanical Properties of Ceramic Materials," I, Journal American Ceramic Society, 41, 6, 189-95, 1958 and II, Journal American Ceramic Society, 42, 8, pp. 288-91, 1959.

3. J. A. Kuszyk and R. C. Bradt, "Influence of Grain Size on Effects of Thermal Expansion Anisotrophy in $MgTi_2O_5$," Journal American Ceramic Society, 56, 8, pp. 420-23, 1973

4. W. R. Manning and O. Hunter, Jr., F. W. Calderwood and D. W. Stacy, "Thermal Expansion of Nb_2O_5," Journal American Ceramic Society, 55 7, pp. 342-47, 1972.

5. H. J. Siebeneck, D. P. H. Hasselman, J. J. Cleveland and R. C. Bradt, "Effect of Microcracking on the Thermal Diffusivity of Fe_2TiO_5," Journal American Ceramic Society, 59 5-6, pp. 239-41, 1976.

6. H. J. Siebeneck, J. J. Cleveland, D. P. H. Hasselman and R.C. Bradt, "Grain-Size-Microcracking Effects on the Thermal Diffusivity of $MgTi_2O_5$," Journal American Ceramic Society, (in press).

7. W. J. Parker, R. J. Jenkins, C. P. Butler and G. L. Abbott, "Flash Method of Determining Thermal Diffusivity, Heat Capacity and Thermal Conductivity," Journal Applied Physics, 32 9, pp. 1679-81, 1961.

8. D. P. H. Hasselman, "Unified Theory of Thermal Shock Fracture Initiation and Crack Propagation in Brittle Ceramics," Journal American Ceramic Society, 52, 11, pp. 600-04, 1969.

9. W. R. Manning, unpublished results.

Figure 1. Scanning electron micrographs of fracture surfaces of aluminum niobate.

Figure 1 (a). Hot Pressed at 1300°C (X6000).

Figure 1. Scanning electron micrographs of fracture surfaces of aluminum niobate.

Figure 1 (b). Sintered at 1350°C (X6000).

Figure 1. Scanning electron micrographs of fracture surfaces of aluminum niobate.

Figure 1 (c). Sintered at 1350°C and Annealed for 24 hours at 1400°C (X3000).

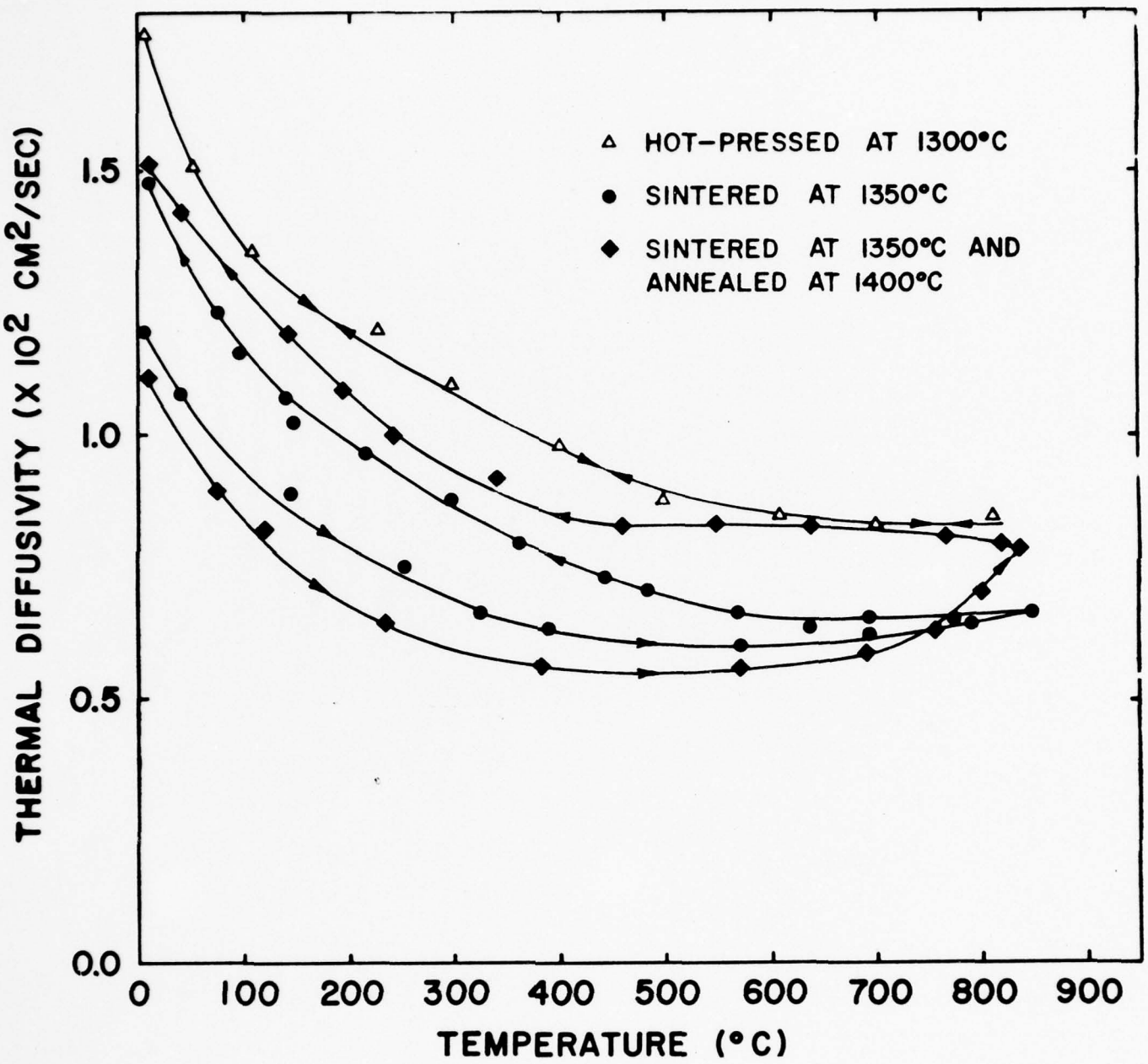

Fig. 2 Thermal diffusivity of polycrystalline aluminum niobate for various heat-treatments.

APPENDIX E

ENHANCED THERMAL STRESS RESISTANCE OF BRITTLE CERAMICS WITH THERMAL CONDUCTIVITY GRADIENT

ENHANCED THERMAL STRESS RESISTANCE OF STRUCTURAL CERAMICS WITH THERMAL CONDUCTIVITY GRADIENT

by

D.P.H. Hasselman

and

G.E. Youngblood

Montana Energy and MHD Research and Development Institute, Inc.
Butte, Montana 59701

ABSTRACT

The hypothesis is presented that the maximum tensile thermal stresses in brittle ceramics can be reduced significantly by a redistribution of the temperature profile by means of a spatially varying thermal conductivity. On the basis of a hollow circular cylinder subjected to radially inward or outward steady-state heat flow, it is shown that indeed such a spatially varying thermal conductivity can lead to significant decreases in magnitude of the maximum tensile thermal stress. Possible techniques of creating such thermal conductivity variations are discussed briefly.

I. INTRODUCTION

Brittle structural ceramics for high-temperature applications are highly susceptible to thermal stress fracture. [1] The incidence of thermal stress fracture can be reduced by the selection of materials with values as low as possible of the coefficient of thermal expansion, Young's modulus of elasticity, Poisson's ratio and emissivity in combination with high values of tensile strength, thermal conductivity and thermal diffusivity. [1] Rapid crack arrest after thermal stress fracture can be promoted by selecting materials with moderate strength, high Young's modulus and high values of fracture energy and which exhibit stable crack propagation. [2] From the point of view of engineering design, thermal stresses can be reduced by decreasing the structure size and developing highly compliant structures with a minimum of external mechanical constraints. [3]

In general the magnitude of thermal stress is governed by both the total temperature difference within the structure and the temperature distribution. [3] Under steady-state or transient heat transfer the temperature distribution is governed by the thermal conductivity and/or thermal diffusivity. This suggests that thermal stress levels can be reduced by altering the temperature distribution simply by developing structures with a spatial variation in thermal conductivity or diffusivity. As far as the present authors are aware, this technique has not been suggested previously. Such spatial variation of thermal conductivity is easily accounted for in thermal stress calculations by numerical methods. It is the purpose of this paper to demonstrate the validity of the proposed method by analytical derivations of thermal stresses under conditions of steady-state heat transfer in structures of simple geometry in which the thermal conductivity has a spatial dependence and all other relevant properties are held invariant.

Major changes in thermal conductivity can be accomplished by introducing lattice defects such as impurities, vacancies [4] or solid-solution alloying additions.[5,6] For any specific material system, if such lattice defects were to cause minor or major changes in properties other than thermal conductivity and their dependence on temperature, such changes can also be incorporated easily in thermal stress calculations using numerical techniques.

In order to quantitatively assess the effect of this single variable, this study will focus on the spatial variation of thermal conductivity only. Specifically, the analysis will be based on a hollow circular cylinder with radially outward and inward steady-state flow.

II. ANALYSIS

A. Hollow cylinder with radially outward heat flow.

An infinitely long hollow circular cylinder with $a \leq r \leq b$, where a and b are the inner and outer radius, resp., is considered. The surface temperature T_b (at $r = b$) is arbitrarily selected as $T_b = 0$. The temperature ΔT at the inner surface (at $r = a$) is the result of a uniform heat flux Q per unit length. Heat flow occurs in the radial direction only. Under steady-state conditions the general expression for heat conduction is

$$Q = - 2\pi r K \, (dT/dr) \tag{1}$$

where K is the thermal conductivity and (dT/dr) is the temperature gradient at radius r.

The dependence of the thermal conductivity on a structural or compositional variable arbitrarily is assumed to be of the form

$$K = K_o (1 + f)^{-1} \qquad f \geq 0 \tag{2}$$

where f is a function of the defect concentration and its effect on the thermal conductivity. As an example consider the effect of 30% chromia alloying on the thermal conductivity of alumina at 200°C. From the data of Matta and Hasselman,[5] f can be deduced to be approximately equal to unity. This corresponds to a decrease in thermal conductivity value from that of a pure alumina of approximately a factor of 2.

By allowing f in Eq. (2) to be a function of r, the spatial dependence of the thermal conductivity can be introduced. Setting $f = f_o$ at $r = a$, f was chosen arbitrarily as

$$f = f_o \, (a/r)^n \tag{3}$$

where n is referred to as the thermal conductivity distribution constant. Equations (2) and (3) together give the spatial dependence of the thermal conductivity. Upon substitution into Eq. (1) and integrating, with the boundary condition that when $r = b$, $T = 0$, Eq. (1) yields the temperature distribution

$$T = \frac{Q}{2\pi K_c} \left\{ \ln\left(\frac{b}{r}\right) + \frac{f_o}{n}\left[\left(\frac{a}{r}\right)^n - \left(\frac{a}{b}\right)^n\right]\right\} \tag{4}$$

Considering that $T = \Delta T$ when $r = a$, Eq. (4) can be re-expressed as

$$T = \Delta T \left\{ \frac{\ln\left(\frac{b}{r}\right) + \frac{f_o}{n}\left[\left(\frac{a}{r}\right)^n - \left(\frac{a}{b}\right)^n\right]}{\ln\left(\frac{b}{a}\right) + \frac{f_o}{n}\left[1 - \left(\frac{a}{b}\right)^n\right]} \right\} \tag{5}$$

The thermal stresses in a hollow cylinder consist of radial, tangential and longitudinal stresses. The tangential and longitudinal stresses have their extremum values and are equal at the inside

or outside surface (r = a,b). For the present study the magnitude of the maximum tensile stress is of interest. For simplicity then, only the longitudinal stress σ_z need be examined.

The general expression for the longitudinal stress[3] in a hollow cylinder is

$$\sigma_z = \frac{\alpha E}{1-\nu}\left\{\frac{2}{b^2-a^2}\int_a^b r\,T(r)\,dr - T(r)\right\} \tag{6}$$

Substitution of Eq. (5) into Eq. (6) yields

$$\sigma_z = \frac{\alpha E \Delta T}{1-\nu}\left\{\frac{\frac{1}{2} - \ln\left(\frac{b}{r}\right) - \frac{a^2}{b^2-a^2}\ln\left(\frac{b}{a}\right) - \frac{f_o}{n}\left(\frac{a}{r}\right)^n - \frac{2f_c b^2}{n(n-2)(b^2-a^2)}\left[\left(\frac{a}{b}\right)^n - \left(\frac{a}{b}\right)^2\right]}{\ln\left(\frac{b}{a}\right) + \frac{f_o}{n}\left[1 - \left(\frac{a}{b}\right)^n\right]}\right\} \tag{7}$$

In order to examine the effect of extreme thermal conductivity gradients on the magnitude of thermal stress, in addition to the above analysis, the spatial dependence of the thermal conductivity was chosen as

$$f = f_0(b/r)^n \tag{8}$$

such that $f = f_0$ at $b = r$. Equation (8) implies that for high values of n, the thermal conductivity at r = a will reach very low values.

Substitution of Eq. (8) and Eq. (2) into Eq. (1), followed by integration of Eq. (1), and again using the boundary condition that T =0 when r = b, yields the temperature distribution

$$T = \frac{Q}{2\pi k_o}\left\{\ln\left(\frac{b}{r}\right) + \frac{f_c}{n}\left[\left(\frac{b}{r}\right)^n - 1\right]\right\} \tag{9}$$

Following the procedure used to obtain Eq. (5), Eq. (9) can be expressed in terms of ΔT as

$$T = \Delta T \left\{ \frac{\ln\left(\frac{b}{r}\right) + \frac{f_o}{n}\left[\left(\frac{b}{r}\right)^n - 1\right]}{\ln\left(\frac{b}{a}\right) + \frac{f_o}{n}\left[\left(\frac{b}{a}\right)^n - 1\right]} \right\} \tag{10}$$

Substitution of Eq. (10) into Eq. (6) yields the longitudinal stress

$$\sigma_z = \frac{\alpha E \Delta T}{1-\nu} \left\{ \frac{\frac{1}{2} - \ln\left(\frac{b}{r}\right) - \frac{a^2}{b^2-a^2}\ln\left(\frac{b}{a}\right) - \frac{f_o}{n}\left(\frac{b}{r}\right)^n + \frac{2 f_o a^2}{n(n-2)(b^2-a^2)}\left[\left(\frac{b}{a}\right)^n - \left(\frac{b}{a}\right)^2\right]}{\ln\left(\frac{b}{a}\right) + \frac{f_o}{n}\left[\left(\frac{b}{a}\right)^n - 1\right]} \right\} \tag{11}$$

B. Hollow cylinder with radially inward heat flow.

An infinitely long hollow cylinder with $a \leq r \leq b$ is again considered. The inside surface temperature T_a (at $r = a$) is taken as $T = 0$. The temperature ΔT at the outer surface (at $r = b$) is the result of a uniform heat flux Q per length of cylinder. Under conditions of steady-state heat flow, the general expression for inward radial heat flow is

$$Q = 2\pi r K \, (dT/dr) \tag{12}$$

The spatial dependence of thermal conductivity is again established by taking f in Eq. (2) arbitrarily as

$$f = f_0 (r/b)^n \tag{13}$$

Substitution of Eq. (13) into Eq. (2) and then into Eq. (12) followed by integration, with the boundary condition that $T = 0$ at $r = a$, yields the temperature distribution

$$T = \frac{Q}{2\pi K_o} \left\{ \ln\left(\frac{r}{a}\right) + \frac{f_o}{n}\left[\left(\frac{r}{b}\right)^n - \left(\frac{a}{b}\right)^n\right] \right\} \tag{14}$$

which can be expressed in terms of ΔT by

$$T = \Delta T \left\{ \frac{\ln\left(\frac{r}{a}\right) + \frac{f_o}{n}\left[\left(\frac{r}{b}\right)^n - \left(\frac{a}{b}\right)^n\right]}{\ln\left(\frac{b}{a}\right) + \frac{f_o}{n}\left[1 - \left(\frac{a}{b}\right)^n\right]} \right\} \qquad (15)$$

As for the previous case of radially outward heat flow, the extremum values of thermal stress can be obtained by considering the longitudinal stress only. Substitution of Eq. (15) into Eq. (6) yields

$$\sigma_z = \frac{\alpha E \Delta T}{1-\nu} \left\{ \frac{-\frac{1}{2} - \ln\left(\frac{r}{a}\right) + \frac{b^2}{b^2-a^2}\ln\left(\frac{b}{a}\right) - \frac{f_o}{n}\left(\frac{r}{b}\right)^n + \frac{2 f_o b^2}{n(n+2)(b^2-a^2)}\left[1 - \left(\frac{a}{b}\right)^{n+2}\right]}{\ln\left(\frac{b}{a}\right) + \frac{f_o}{n}\left[1 - \left(\frac{a}{b}\right)^n\right]} \right\} \qquad (16)$$

III. RESULTS AND DISCUSSION

Figure 1 shows the calculated values of maximum tensile thermal stress (occuring at r = b) for the hollow cylinder with outward radial heat flow and a thermal conductivity with a spatial distribution described by Eqs. (2) and (3). The curves are drawn for a range of f_o values and three cases of relative wall thickness (i.e., b/a ratio). The maximum thermal stress values for a uniform thermal conductivity distribution (i.e., for $f_o = 0$) are also indicated by a dashed line for each case.

It is clearly evident from these calculated data that a thermal conductivity gradient can lead to significant decreases in the magnitude of tensile thermal stresses. The effect is most pronounced for the thick-walled cylinder, where the reduction in thermal stress level is of the order of three for the range of f_o and n values considered. The amount of reduction in thermal stress levels which can be obtained decreases with decreasing b/a ratio. Nevertheless, even for b/a = 1.1 the reduction is sufficient to be of practical engineering significance.

In Fig. 1 for b/a = 10, it may be noted that the minimum in tensile thermal stress occurs at intermediate values of n. This effect generally would be expected from the specific thermal conductivity distribution resulting from Eqs. (2) and (3). At very low values of n the thermal conductivity throughout the thickness is approximately equal to the thermal conductivity at r = a. This results in a relatively uniform thermal conductivity and little change in thermal stress levels. At very high values of n the thermal conductivity approaches the original conductivity K_o throughout the thickness, with the exception at r = a. Again, there is little effect on the magnitude of the tensile thermal stress. Only at intermediate values of n, for which the relative change in thermal conductivity exhibits the greatest degree of non-uniformity, will a large reduction in the magnitude of the maximum tensile thermal stress occur. Although this effect is clearly evident for b/a = 10, a similar minimum also is expected for b/a = 1.1 and 2 at values of n higher than those indicated in Fig. 1.

The minimum value of the thermal conductivity distribution for the data shown in Fig. 1, $K = K_o / (1 + f_o)$, occurs at r = a. With increasing r, K approaches K_o more or less rapidly depending on the value of n. In contrast for the thermal conductivity distribution given by Eqs. (2) and (8), $K = K_o / (1 + f_o)$ is now the maximum thermal conductivity and occurs at r = b. Again depending on the value of n chosen, the relative thermal conductivity decreases more and more rapidly as r decreases. This results in sharply contrasting thermal stress levels as indicated in Fig. 2. In this figure the data show that with increasing n values (i.e., lower thermal conductivity at r = a), the thermal stress levels can be reduced by up to an order of magnitude.

AD-A045 527 MONTANA ENERGY AND MHD RESEARCH AND DEVELOPMENT INST --ETC F/G 11/2
THERMAL CONDUCTIVITY AND DIFFUSIVITY OF ENGINEERING CERAMICS.(U)
JUN 77 D P HASSELMAN, G E YOUNGBLOOD N00014-76-C-0884

UNCLASSIFIED NL

2 OF 2
ADA045 527

END
DATE FILMED
11-77
DDC

END
DATE FILMED
11-77
DDC

In Fig. 2 the curves for the various b/a values were extended to include a value of thermal conductivity at r = a which is 0.001 of the value at r = b and which may represent an exaggerated case. However, of interest to note is that at these thermal conductivity ratios, the compressive thermal stress at r = a equals $-\alpha E\Delta T/(1-\nu)$; whereas the maximum tensile thermal stress at r = b approaches zero. This automatically suggests for the specific heat transfer conditions selected for this analysis that the application of a thin coating of a low thermal conductivity material at the hot surface can be very effective in increasing the thermal stress resistance of the coated ceramic. The physical reason for this is that for a given value of ΔT across the cylinder wall most of the temperature difference occurs in the low thermal conductivity coating. This causes a very low temperature gradient and low tensile thermal stresses in the outer cooler regions of the body.

Figure 3 indicates values of the maximum tensile thermal stress at r = a for the hollow cylinder subjected to inward radial heat flow and the thermal conductivity distribution resulting from Eqs. (2) and (13). With the exception that the magnitude of stress reduction obtainable with a thermal conductivity gradient appears to be somewhat less, effects qualitatively similar to the results for the radial outward heat flow shown in Fig. 1 are noted.

The results shown in Figs. 1, 2, and 3 offer firm evidence for the validity of the hypothesis that thermal conductivity gradients can be used to advantage in improving thermal stress resistance. Although the results presented were derived for a specific geometry under conditions of steady-state heat flow, they should have general applicability for

other geometries and perhaps transient heat flow as well.

The present analysis, for convenience reasons, was based on a spatial decrease in thermal conductivity. Whether a decrease or increase in conductivity was employed is immaterial, since the magnitude of thermal stress for the heat flow conditions chosen (i.e., fixed ΔT) is a function only of the relative thermal conductivity distribution. The choice of selectively increasing or decreasing thermal conductivity will depend on whether the specific geometry under consideration should function as a good thermal insulator or a good thermal conductor.

In principle the concept of using a thermal conductivity gradient for reducing thermal stress levels can also be used to decrease thermal stresses which arise from the temperature dependence of the thermal conductivity. Such a situation can arise, for instance, under conditions of a steady-state heat flow across a flat plate. In this case for a thermal conductivity independent of temperature, the temperature distribution will be linear and zero thermal stress results. However, as shown by Ganguly and Hasselmar [6] for aluminum oxide, the temperature dependence of the thermal conductivity causes deviations in linearity of the temperature distribution which results in appreciable levels of thermal stress. By means of a suitable thermal conductivity gradient the temperature dependence of the thermal conductivity can be offset to result in zero thermal stress. For the flat plate of alumina considered by Ganguly and Hasselman [6] where the thermal conductivity has a reciprocal temperature dependence, the temperature distribution can be linearized by decreasing the thermal conductivity at the cooler parts of the plate or increasing the thermal conductivity in the hotter sections of the plate.

The specific technique for modifying the thermal conductivity

distribution will depend on the material system under consideration. For crystalline materials the thermal conductivity gradient can be established by solid-solution or impurity gradients. By means of selective phase additions a thermal conductivity gradient also can be easily established in a similar way. A spatially varying degree of crystallization in glass-ceramics should prove to be very effective in producing the required thermal conductivity gradients in view of the large relative difference in thermal conductivity of glassy and crystalline materials. The use of second phases, which alter properties in addition to thermal conductivity, can be used to even greater advantage. Alloying ceramics with metals in many cases can improve thermal conductivity and decrease such properties as Young's modulus of elasticity and the coefficient of thermal expansion. Graded structures of such cermets may have exceptional thermal stress resistance. Very large thermal conductivity gradients can result by changing the heat conduction mechanism within a material from phonon transport with relatively low thermal conductivity to electron transport with a much higher thermal conductivity. Graded porous structures also may be used to considerable advantage. Clearly each thermal stress situation should be examined individually to determine the most appropriate technique of producing a thermal conductivity gradient.

In summary, the present study demonstrates that modification of the temperature distribution within a ceramic structure subjected to steady-state heat flow by means of a thermal conductivity gradient can lead to substantial decreases in tensile thermal stress levels.

ACKNOWLEDGMENTS

This analysis was carried out as part of a larger research program on the thermal conductivity and diffusivity of engineering ceramics sponsored by the Office of Naval Research under contract N00014-76-C-0884. Mike Tuck and Ken Tucker are acknowledged for their help in carrying out the calculations of thermal stresses with the aid of a computer program.

REFERENCES

1. W. D. Kingery, H. K. Bowen and D. R. Uhlman, Introduction to Ceramics, 2nd Ed., John Wiley, New York, 1976.

2. D. P. H. Hasselman, "Unified Theory of Thermal Shock Fracture Initiation and Crack Propagation in Brittle Ceramics," Journal American Ceramic Society, 52, 11, pp. 600-04, 1969.

3. B. A. Boley and J. H. Weiner, Theory of Thermal Stresses, John Wiley, New York, 1960.

4. H. J. Siebeneck, W. P. Minnear, R. C. Bradt and D. P. H. Hasselman, "Thermal Diffusivity of Nonstoichiometric Titanium Dioxide," Journal American Ceramic Society, 59, pp. 84, 1976.

5. J. E. Matta and D. P. H. Hasselman, "The Thermal Diffusivity of Al_2O_3-Cr_2O_3 Solid Solutions," Journal American Ceramic Society, 58, p. 458, 1975.

6. B. Ganguly, K. R. McKinney and D. P. H. Hasselman, "Thermal Stress Analysis of Flat Plate with Temperature Dependent Thermal Conductivity," Journal American Ceramic Society, 58, p. 455-56, 1975.

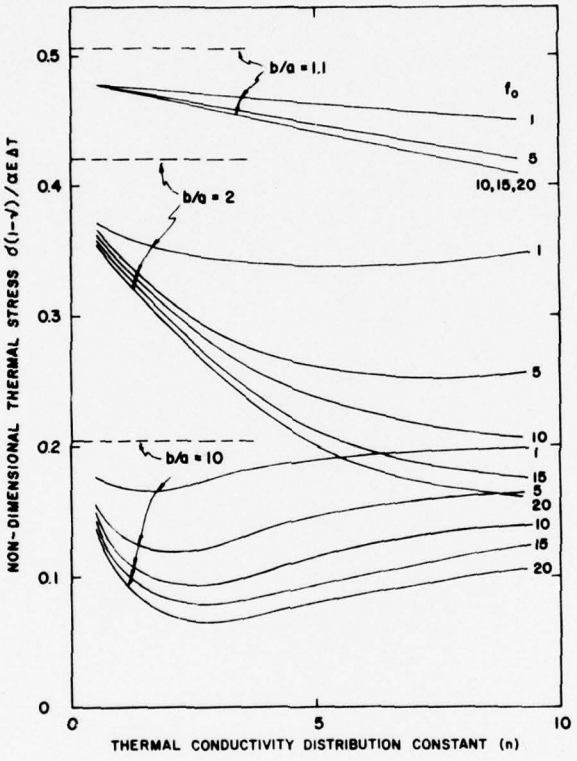

Fig. 1. Calculated values of maximum tensile thermal stress for a hollow cylinder with outward radial heat flow and a thermal conductivity with a spatial distribution described by Eqs. (2) and (3) (——— solid line) and a uniform spatial distribution (- - - dashed line).

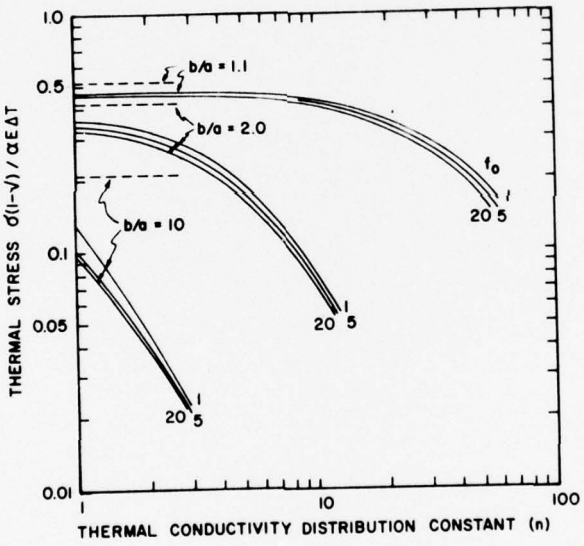

Fig. 2. Calculated values of maximum tensile thermal stress for a hollow cylinder with outward radial heat flow and a thermal conductivity with a spatial distribution described by Eqs. (2) and (8) (——— solid lines) and a uniform spatial distribution (- - - dashed lines).

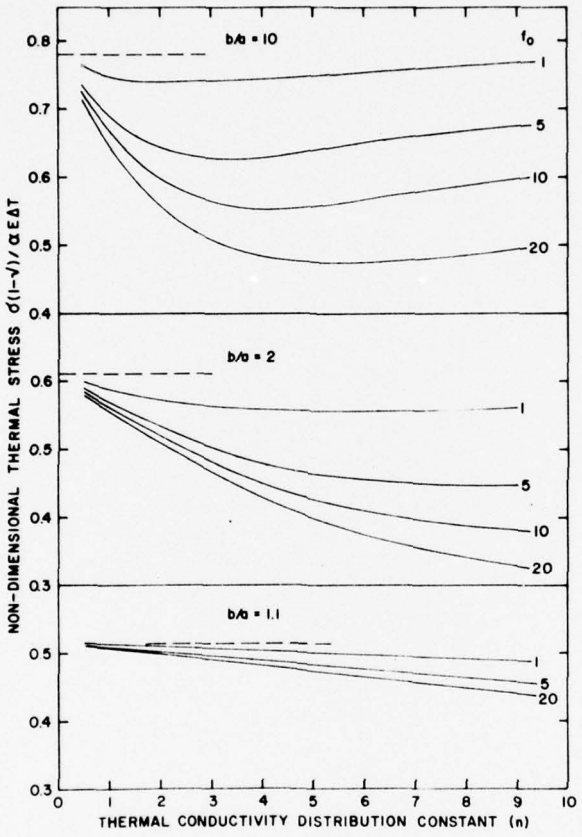

Fig. 3. Calculated values of maximum tensile thermal stress for a hollow cylinder with inward radial heat flow and a thermal conductivity with a spatial distribution described by Eqs. (2) and (13) (——— solid lines) and a uniform spatial distribution (- - - dashed lines).

APPENDIX F

EFFECT OF CRYSTALLIZATION ON THE THERMAL DIFFUSIVITY OF A MICA GLASS-CERAMIC

EFFECT OF CRYSTALLIZATION ON THE THERMAL DIFFUSIVITY OF A MICA GLASS-CERAMIC

by

H.J. Siebeneck,* K. Chyung,+ D.P.H. Hasselman,‡ G.E. Youngblood‡

* University of Maryland, College Park, MD, 20740
\+ Corning Glass Works, Corning, NY, 14830
‡ The Montana Energy and MHD Research and Development Institute, Inc. Butte, MT, 59701

EFFECT OF CRYSTALLIZATION OF THE THERMAL DIFFUSIVITY OF A MICA GLASS-CERAMIC

H.J. Siebeneck, K. Chyung, D.P.H. Hasselman, and G. E. Youngblood

The conduction of heat in dense dielectric materials occurs primarily by phonon and photon transport. For a given material, phonon heat transfer is strongly controlled by the perfection of the crystal structure, such as the degree of crystallinity [1] or the number of foreign atoms, [2] vacancies, [3] and other phonons. [4] Photon transport is strongly affected by the emission and absorption characteristics [5] of the material itself as well as by the scattering [6] at optical discontinuities such as pores or grain boundaries [7] in optically inhomogeneous materials and at inclusions with refraction and transmission properties other than those of the host matrix. [6] The thermal conductivities due to phonon and photon transport generally show a negative and positive temperature dependence, respectively. [1] The temperature dependence for a given material will depend on the relative contributions of the phonon and photon heat transfer to the total thermal conductivity.

Many of the structural and compositional features which affect phonon and photon heat transfer are a function of the fabrication history of the material. As a result, for a given material a degree of control exists over the thermal conductivity and its temperature dependence. This hypothesis is illustrated by experimental data for the thermal diffusivity and conductivity of a glass-ceramic subjected to a series of heat treatments.

The glass-ceramic chosen for this study was a fluorophlogopite mica glass-ceramic* described in detail elsewhere. [8] The high degree of machinability of this glass-ceramic assisted in the preparation of specimens.

* Code 9658, Corning Glass Works, Corning, NY

The glass-ceramic, originally in a two-phase glassy state was partially crystallized by heat treatment for 4 hours at 800°C, 850°C, 900°C, and 950°C followed by replication electron microscopy and density measurements. The thermal diffusivity over the temperature range of 25°C to 800°C was measured by the laser-flash diffusivity technique [9] using equipment described in detail elsewhere. [2] In this measurement the transient temperature of the specimen was monitored by a thermocouple attached with a ceramic cement to a 0.1 inch thick disc-shaped specimen.

Figure 1a shows the microstructure of the original as-cooled glass which shows evidence for liquid-liquid phase separation essential for the crystal nucleation. Figures 1b, 1c, and 1d show the structure of the glass crystallized at 800°C, 900°C, and 950°C. As reported in detail by Chyung *et al.*, [8] the glass undergoes a complex three-stage crystallization sequence on heating that eventually leads to *fluorophlogopite mica* formation. Briefly the stages are (a) heterogeneous nucleation of chondrodite-like crystals and their growth into the matrix above 650°C followed by, (b) the recrystallization of the chondrodite to norbergite above 750°C, and finally (c) epitaxial growth of phlogopite crystals on norbergite above 850°C. Table I gives the densities and fractional crystallization content which were estimated from the electron micrographs.

Figure 2 illustrates the temperature dependence of the thermal diffusivity on crystallization temperature. These results clearly indicate that the crystallization causes an appreciable increase in the thermal diffusivity and a large change in its temperature dependence as well. These observations can be explained qualitatively in terms of mechanisms of heat transfer in solids.

In general, the thermal conductivity (k) of a solid material controlled by a given mechanism can be expressed

$$k = 1/3\ sv\ell \qquad (1)$$

where s is the contribution of the heat transfer mechanism to the specific heat per unit volume, v is the velocity of the carrier for the particular mechanism of heat transfer and ℓ is the corresponding mean free path of the carrier.

The thermal diffusivity (α) is defined by

$$\alpha = k/\rho c \qquad (2)$$

where ρ is the density and c is the specific heat per unit mass with $\rho c = s$. Substitution of Equation (1) for k in Equation (2) yields

$$\alpha = 1/3\ v\ell \qquad (3)$$

Equation (3) indicates that the thermal diffusivity can be expressed in terms of carrier mean free path and velocity only.

In the present mica glass-ceramics heat conduction occurs primarily by phonon and photon transport processes. Phonon transport will predominate at the lower temperatures and will exhibit a negative temperature dependence; photon heat transfer with its positive temperature dependence will make an increased contribution to the thermal diffusivity at the higher temperatures. The two contributing mechanisms and their temperature dependence will result in a U-shaped form of the α vs. temperature (T) curves, indeed as observed for the present data.

The major part of the increase in the thermal diffusivity at the lower temperatures most likely can be attributed to an increase in the mean free path and velocity within the crystalline phase, which results in an increase in the overall thermal diffusivity of the glass-crystal composite. The amount of increase in thermal diffusivity due to the crystallization diminishes with increasing temperature. This can be attributed to a reduction of the relative contribution of photon heat transfer to the total thermal conductivity. This is the result of increased photon scattering (i.e., reduction in photon mean

free path) at the crystallite-glass phase boundaries. The shift in the minima of the α vs. T curves with increased crystallization temperature also is indicative of this effect. The near coincidence of α vs. T at 800°C for the three highest crystallization temperatures suggests that the presence of the crystalline phase in fact has caused a reduction in the absolute amount of photon heat transfer approximately equal to the increase due to phonon heat transfer. A quantitative theoretical estimate of the present data in terms of phonon and photon transport contributions and scattering processes is expected to be of considerable complexity due particularly to the irregular crystalline particle shape and the expected anisotropic behavior of the mica-phase.

Nevertheless, the present data illustrate that the heat conduction properties of dielectric materials can be controlled, at least within some limits, by microstructural and/or compositional modifications. This in particular is the case for glass-ceramics in view of their wide range of possible modifications as well as the general ease of process control for these materials. For instance, the thermal diffusivity of the present fluorophlogopite mica glass-ceramics are about a factor of three lower than the corresponding values for Pyroceram C-9606 or C-9608.* [10]

* Corning Glass Works, Corning, NY

Acknowledgments

The measurements of thermal diffusivity and manuscript preparation were carried out as part of a larger research program on the thermal conductivity and diffusivity of engineering ceramics, supported by the Office of Naval Research under agreement No. N00014-76-C-0884. Electron micrography and density measurements were performed at the Corning Glass Works.

REFERENCES

1. W. D. Kingery, Introduction to Ceramics, 1st edition, John Wiley and Sons, Inc., New York, p. 489, 1960.

2. J. E. Matta and D. P. H. Hasselman, "Thermal Diffusivity of Al_2O_3-Cr_2O_3 Solid Solutions," Journal American Ceramic Society, 58, p. 458, 1975.

3. H. J. Siebeneck, W. P. Minnear, D. P. H. Hasselman, and R. C. Bradt, "Thermal Diffusivity of Non-Stoichiometric Titanium Dioxide," Journal American Ceramic Society, 59, p.84, 1976.

4. Charles Kittel, Introduction to Solid State Physics, 3rd edition, John Wiley and Sons, Inc., New York, p. 187, 1966.

5. Robert Gardon, "A Review of Radiant Heat Transfer in Glass," Journal American Ceramic Society, 44, 7, p. 305, 1961

6. E. M. Sparrow and R. D. Cess, Radiation Heat Transfer, revised edition, Brooks/Cole Publishing Co., Belmont, California, pp. 12-31, 1970.

7. D. W. Lee and W. D. Kingery, "Radiation Energy Transfer and Thermal Conductivity of Ceramic Oxides," Journal American Ceramic Society, 43, 11, p. 544, 1960.

8. K. Chyung, G. H. Beall, and D. G. Grossman, "Fluorophlogopite Mica Glass-Ceramics," Tenth Inst. Congress of Glass, Kyoto Japan, (The Ceramic Society of Japan), pp. 14-33, July 1974.

9. W. J. Parker, R. J. Jenkins, C. P. Butler, and G. L. Abbott, "Flash Method of Determining Thermal Diffusivity, Heat Capacity, and Thermal Conductivity," Journal Applied Physics, 32 9, p. 1679, 1961.

10. Y. S. Touloukian, R. W. Powell, C. Y. Ho, and M. C. Nicolaou, Thermal Diffusivity, Volume 10 of Thermophysical Properties of Matter Series, IFK/Plenum, New York, p. 581, 1973.

Table I. Density and Crystallinity of Mica Glass-Ceramic

Heat Treatment	Density (gr/cm^3)	Vol. % Crystallinity
1) Glass (as-cooled)	2.486	0
2) 800°C-4 hrs.	2.505	40
3) 850°C-4 hrs.	2.511	40-45
4) 900°C-4 hrs.	2.543	40-50
5) 950°C-4 hrs.	2.542	45-50

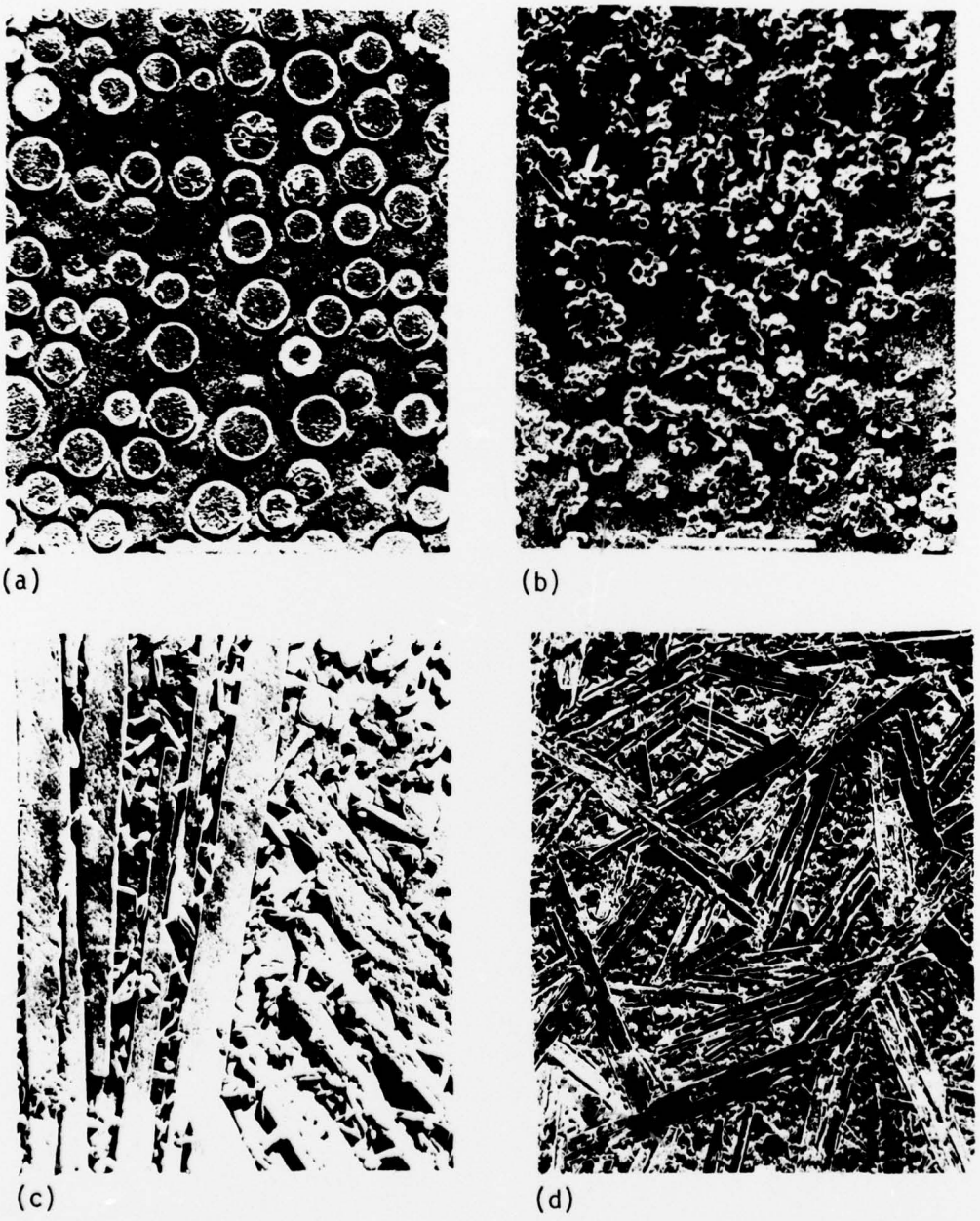

Figure 1. Electron replication micrographs of crystallized mica glass-ceramics. (a) as-cooled glass and glass crystallized at (b) 800°C, (c) 900°C, and (d) 950°C. Bar indicates one micron.

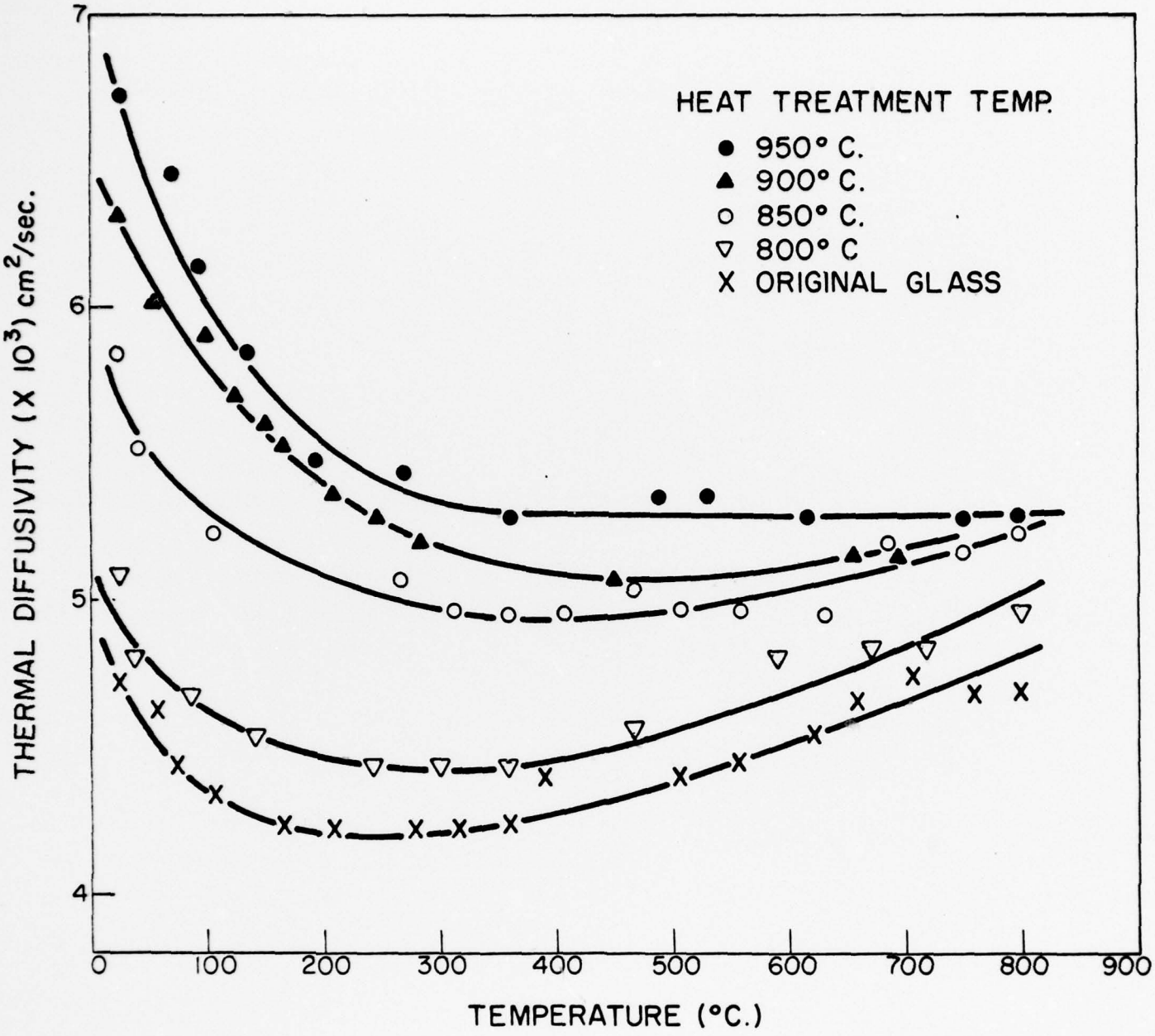

Figure 2. Effect of crystallization at various temperatures for 4 hours on the thermal diffusivity of a mica glass-ceramic

BASIC DISTRIBUTION LIST

Technical and Summary Reports

Organization	No. of Copies
Defense Documentation Center Cameron Station Alexandria, Virginia 22314	(12)
Office of Naval Research Department of the Navy Arlington, Virginia 22217	
Attn: Code 471	(3)
Code 105	(6)
Code 470	(1)
Director Office of Naval Research Branch Office 495 Summer Street Boston, Massachusetts 02210	(1)
Director Office of Naval Research Branch Office 536 South Clark Street Chicago, Illinois 60605	(1)
Office of Naval Research San Francisco Area Office 760 Market Street Room 447 San Francisco, California 94102	(1)
Naval Research Laboratory Washington, DC 20390	
Attn: Code 6000	(1)
Code 6100	(1)
Code 6300	(1)
Code 6400	(1)
Code 2627	(6)
Code 2629	(6)
Attn: Mr. F. S. Williams Naval Air Development Center Code 302 Warminister, Pennsylvania 18974	(1)
Naval Air Propulsion Test Center Trenton, New Jersey 08628	
Attn: Library	(1)

Organization	No. of Copies
Air Force Materials Lab (LA) Wright-Patterson AFB Dayton, Ohio 45433	(1)
Naval Weapons Laboratory Dahlgren, Virginia 22448 Attn: Research Division	(1)
Naval Construction Batallion Civil Engineering Laboratory Port Hueneme, California 93043 Attn: Materials Division	(1)
Naval Electronic Laboratory Center San Diego, California 92152 Attn: Electronic Materials Science Division	(1)
Naval Missile Center Materials Consultant Code 3312-1 Point Mugu, California 93041	(1)
Commanding Officer Naval Ordnance Laboratory White Oak Silver Spring, Maryland 20910 Attn: Library	(1)
Naval Ship R&D Center Materials Department Annapolis, Maryland 21402	(1)
Naval Undersea Center San Diego, California 92132 Attn: Library	(1)
Naval Underwater System Center Newport, Rhode Island 02840 Attn: Library	(1)
Naval Weapons Center China Lake, California 93555 Attn: Library	(1)
Naval Postgraduate School Monterey, California 93940 Attn: Materials Sciences Dept.	(1)

Organization	No. of Copies
Naval Air Systems Command Washington, DC 20360 Attn: Code 52031 Code 52032 Code 320	 (1) (1) (1)
Naval Sea System Command Washington, DC 20362 Attn: Code 035	 (1)
Naval Facilities Engineering Command Alexandria, Virginia 22331 Attn: Code 03	 (1)
Scientific Advisor Commandant of the Marine Corps Washington, DC 20380 Attn: Code AX	 (1)
Naval Ship Engineering Center Department of the Navy Washington, DC 20360 Attn: Director, Materials Sciences	 (1)
Army Research Office Box CM, Duke Station Durham, North Carolina 27706 Attn: Metallurgy & Ceramics Div.	 (1)
Army Materials and Mechanics Research Center Watertown, Massachusetts 02172 Attn: Res. Programs Office (AMXMR-P)	 (1)
Commanding General Department of the Army Frankford Arsenal Philadelphia, Pennsylvania 19137 Attn: ORDBA-1320	 (1)
Office of Scientific Research Department of the Air Force Washington, DC 20333 Attn: Solid State Div. (SRPS)	 (1)
Aerospace Research Labs Wright Patterson AFB Dayton, Ohio 45433	 (1)
NASA Headquarters Washington, DC 20546 Attn: Code RRM	 (1)

Organization	No of Copies
NASA Lewis Research Center 21000 Brookpark Road Cleveland, Ohio 44135 Attn: Library	(1)
National Bureau of Standards Washington, DC 20234 Attn: Metallurgy Division Inorganic Materials Division	(1) (1)
Energy Research and Development Agency Washington, DC 20545 Attn: Metals & Materials Branch	(1)
Defense Metals & Ceramics Information Center Battelle Memorial Institute 505 King Avenue Columbus, Ohio 43201	(1)
Director Ordnance Research Laboratory P.O. Box 30 State College, Pennsylvania 16801	(1)
Director Applied Physics Lab. University of Washington 1013 Northeast Fortieth Street Seattle, Washington 98105	(1)
Metals and Ceramics Division Oak Ridge National Laboratory P.O. Box X Oak Ridge, Tennessee 37830	(1)
Los Alamos Scientific Lab. P.O. Box 1663 Los Alamos, New Mexico 87544 Attn: Report Librarian	(1)
Argonne National Laboratory Metallurgy Division P.O. Box 229 Lemont, Illinois 60439	(1)
Brookhaven National Laboratory Technical Information Division Upton, Long Island New York 11973 Attn: Research Library	(1)

Oragnization	No. of Copies
Library Building 50 Room 134 Lawrence Berkeley Laboratory Berkeley, California 94704	(1)
Mr. Sidney Brown Resident Representative Office of Naval Research University of Pennsylvania The Moore School of Electrical Engineering 200 South 33rd Street Philadelphia, Pennsylvania 19104	(1)

SUPPLEMENTARY DISTRIBUTION LIST

Technical and Summary Reports

Professor R. Roy
Pennsylvania State University
Materials Research Laboratory
University Park, Pennsylvania
16802

Professor R. H. Doremus
Rensselaer Polytechnical Institute
Troy, New York 12181

Professor D. H. Whitmore
Northwestern University
Department of Metallurgy
Evanston, Illinois 60201

Professor G. R. Miller
University of Utah
Department of Ceramic Engineering
Salt Lake City, Utah 84112

Professor J. A. Pask
University of California
Department of Mineral
Technology
Berkeley, California 94720

Dr. T. D. Chikalla
Battelle Northwest
Ceramics and Graphite Section
P. O. Box 999
Richland, Washington 99352

Professor D. Turnbull
Harvard University
Division of Engineering and
Applied Science
Pierce Hall
Cambridge, Massachusetts 02100

Dr. P. D. Wilcox
Division 2521
Sandia Laboratories
Albuquerque, New Mexico 87115

Dr. T. Vasilos
AVCO Corporation
Research and Advanced
Development Division
201 Lowell Street
Wilmington, Mass. 01887

Mr. I. Berman
Army Materials and Mechanics
Research Center
Waterton, Massachusetts 02171

Dr. H. A. Perry
Naval Ordnance Laboratory
Code 230
Silver Spring, Maryland 20910

Dr. F. F. Lange
Westinghouse Electric Corp.
Research Laboratories
Pittsburgh, Pennsylvania 15235

Dr. Paul Smith
Naval Research Laboratory
Crystals Branch, Code 6430
Washington, DC 20390

Professor H. A. McKinstry
Pennsylvania State University
Materials Research Laboratory
University Park, Pennsylvania 16802

Dr. A. R. C. Westwood
Martin-Marietta Laboratories
1450 South Rolling Road
Baltimore, Maryland 21227

Professor T. A. Litovitz
Catholic University of America
Physics Department
Washington, DC 20017

Dr. R. J. Stokes
Honeywell, Inc.
Corporate Research Center
500 Washington Ave., South
Hopkins, Minnesota 55343

Dr. Harold Liebowitz
Dean of Engineering
George Washington University
Washington, DC 20006

Dr. H. Kirchner
Ceramic Finishing Company
P.O. Box 498
State College, Pennsylvania
16801

Professor A. H. Heuer
Case Western Reserve University
University Circle
Cleveland, Ohio 44106

Dr. E. E. Niesz
Battelle Memorial Institute
505 King Avenue
Columbus, Ohio 43201

Dr. F. A. Kroger
University of Southern
California
University Park
Los Angeles, California 90007

Dr. S. M. Wiederhorn
Inorganic Materials Division
National Bureau of Standards
Washington, DC 20234

Dr. C. O. Hulse
United Aircraft Research Labs
United Aircraft Corporation
East Hartford, Connecticut
06108

Dr. R. M. Haag
Space Systems Division
AVCO Corporation
Lowel Industrial Park
Lowell, Massachusetts 01851

Mr. Charles L. LeBlanc
Naval Underwater Systems Center
Newport, Rhode Island 02840

Stanford University
Department of Materials Sciences
Stanford, California 94305

Dr. R. K. MacCrone
Department of Materials Engineering
Rensselaer Polytechnic Institute
Troy, New York 12181

Dr. D. C. Mattis
Belfer Graduate School of Science
Yeshiva University
New York, New York 10033

Professor R. B. Williamson
College of Engineering
University of California
Berkeley, California 94720

Professor R. W. Gould
Department of Metallurgical and
Materials Engineering
University of Florida
Gainesville, Florida 32601

Professor V. S. Stubican
Department of Materials Science
Ceramic Science Section
Pennsylvania State University
University Park, Pennsylvania 16802

Dr. R. C. Anderson
General Electric R & D Center
P.O. Box 8
Schenectady, New York 12301

The Library
Attention: Assistant Librarian
(Technical Reference)
State University of New York
College of Ceramics at Alfred University
Alfred, New York 14802

Professor M. H. Manghnani
University of Hawaii
Hawaii Institute of Geophysics
2525 Correa Road
Honolulu, Hawaii 96822

Dr. Marvin Hass
Naval Research Laboratory
Code 6408
Washington, DC 20375

Dr. N. N. Ault
Norton Company
1 New Bond St.
Worcester, Massachusetts 01601

Dr. E. A. Bush
Ceramics Research
Corning Glass Works
Corning, New York 14830

Professor P. J. Gielisse
Department of Chemical Engineering
University of Rhode Island
Kingston, Rhode Island 02881

Dr. M. O. Marlowe
General Electric Company
1900 South Tenth St.
San Jose, California 95125

Dr. M. Noone
General Electric Company
Space Sciences Laboratory
Room M9539 P.O. Box 8555
Philadelphia, Pennsylvania 19101

Dr. R. Penty
Fiber Materials Inc.
Biddeford Industrial Park
Biddeford, Maine 04005

Dr. B. Rossing
Westinghouse Research Laboratories
Beulah Road
Pittsburgh, Pennsylvania 15235

Dr. R. Ruh
Air Force Materials Lab.
Wright-Patterson Air Force Base
Dayton, Ohio 45433

Dr. J. E. Doherty
Materials Engineering and
Research Laboratory
Pratt and Whitney Aircraft Corp
Middletown Plant
Middletown, Connecticut 06457

Dr. R. N. Katz
Army Mechanics and Materials
Research Center
Watertown, Massachusetts 02172

Dr. R. C. Bradt
201 Mineral Ind. Building
Pennsylvania State University
University Park, Pennsylvania 16802

Mr. W. B. Crandall
Alfred University
Alfred, New York 14802

Dr. B. G. Koepke
Honeywell Corporate Research Center
10701 Lyndale Avenue
Bloomington, Minnesota 55420

Dr. P. E. D. Morgan
Franklin Institute
Philadelphia, Pennsylvania 19103

Professor E. D. Whitney
Department of Materials Science and
Engineering
University of Florida
Gainesville, Florida 32611

Dr. R. C. Rossi
Materials Sciences Division
Aerospace Corporation
P.O. Box 95085
Los Angeles, California 90045

Dr. J. T. A. Roberts
Electric Power Research Institute
3412 Hillview Ave.
P.O. Box 10412
Palo Alto, California 94304

Dr. W. Plummer
Research and Development
Corning Glass Works
Corning, New York 14830

Dr. Jack Hansen
General Electric Company
Space Sciences Laboratory
P.O. Box 8555
Philadelphia, Pennsylvania 19101

Dr. W. R. Manning
Champion Spark Plug Company
20000 Conner Ave.
Detroit, Michigan 48234

Dr. K. Chueng
Research and Development
Corning Glass Works
Corning, New York 14830

Mr. M. Berberian
Department of Materials Science
and Engineering
The University of Utah
Salt Lake City, Utah 84112

Dr. G. K. Bansal
Battelle
505 King Avenue
Columbus, Ohio 43201

Dr. James D. Buch
Prototype Development Assoc. Inc.
1740 Garry Avenue, Suite 201
Santa Ana, California 92705

Professor L. E. Cross
The Pennsylvania State University
Materials Research Laboratory
University Park, Pennsylvania 16802

Ms. M. E. Gulden
Solar
Division of International Harvester
Company
P.O. Box 951
2200 Pacific Highway
San Diego, California 92112

Dr. Ronald E. Loehman
University of Florida
Ceramics Division
Gainesville, Florida 32601

Mr. John Norbutas
Civil Engineering Laboratory
Naval Construction Battalion Center
Port Hueneme, California 93043

Mr. Roy Rice
Naval Research Laboratory
Code 6360
Washington, DC 20375

Dr. B. A. Wilcox
Ceramics Program, Room 336
Metallurgy and Materials Section
Division of Materials Research
National Science Foundation
Washington, DC 20550

Dr. Richard E. Engdahl, President
Deposits and Composites Inc.
1821 Michael Faraday Drive
Reston, Virginia 22090

Dr. H. E. Bennett
Naval Surface Weapons Center
Research Department Code 601
China Lake, California 93555

Dr. R. J. Charles
General Electric Company
Research and Development Center
Schenectady, New York 12301

Dr. Anthony G. Evans
Rockwell International Science
Center
1049 Camino Dos Rios
Thousand Oaks, California 91360

Dr. James Lankford, Jr.
Southwest Research Institute
8600 Culebra Road
San Antonio, Texas 78284

Professor P. M. Macedo
The Catholic University of America
Washington, DC 20017

Professor R. M. Rose
Department of Metallurgy
Massachusetts Institute of
Technology
Cambridge, Massachusetts 02139

Mr. Arthur I. Braunstein
Hughes Research Laboratories
3011 Malibu Canyon Road
Malibu, California 90265

Dr. Ram Natesh
Materials Research, Inc.
1380 East South Temple St.
Salt Lake City, Utah 84102

Dr. David Godfrey
Admiralty Materials Laboratory
Fulton Heath, Poole Dorset
United Kingdom